CHAPTER

4

FLUID KINEMATICS

Fluid kinematics deals with describing the motion of fluids without necessarily considering the forces and moments that *cause* the motion. In this chapter, we introduce several kinematic concepts related to flowing fluids. We discuss the *material derivative* and its role in transforming the conservation equations from the *Lagrangian description of fluid flow* (following a *fluid particle*) to the *Eulerian description of fluid flow* (pertaining to a *flow field*). We then discuss various ways to visualize flow fields—*streamlines*, *streaklines*, *pathlines*, *timelines*, and optical methods *schlieren* and *shadowgraph*—and we describe three ways to plot flow data—*profile plots*, *vector plots*, and *contour plots*. We explain the four fundamental kinematic properties of fluid motion and deformation—*rate of translation*, *rate of rotation*, *linear strain rate*, and *shear strain rate*. The concepts of *vorticity*, *rotationality*, and *irrotationality* in fluid flows are also discussed. Finally, we discuss the *Reynolds transport theorem* (*RTT*), emphasizing its role in transforming the equations of motion from those following a *system* to those pertaining to fluid flow into and out of a *control volume*. The analogy between material derivative for infinitesimal fluid elements and RTT for finite control volumes is explained.

OBJECTIVES

When you finish reading this chapter, you should be able to

■ Understand the role of the material derivative in transforming between Lagrangian and Eulerian descriptions

■ Distinguish between various types of flow visualizations and methods of plotting the characteristics of a fluid flow

■ Have an appreciation for the many ways that fluids move and deform

■ Distinguish between rotational and irrotational regions of flow based on the flow property vorticity

■ Understand the usefulness of the Reynolds transport theorem

FIGURE 4–1
With a small number of objects, such as billiard balls on a pool table, individual objects can be tracked.
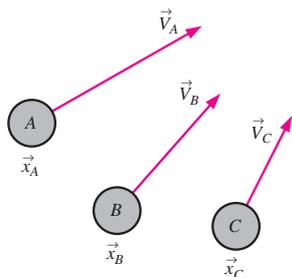
FIGURE 4–2
In the Lagrangian description, one must keep track of the position and velocity of individual particles.

4–1 ▪ LAGRANGIAN AND EULERIAN DESCRIPTIONS

The subject called **kinematics** concerns the study of *motion*. In fluid dynamics, *fluid kinematics* is the study of how fluids flow and how to describe fluid motion. From a fundamental point of view, there are two distinct ways to describe motion. The first and most familiar method is the one you learned in high school physics class—to follow the path of individual objects. For example, we have all seen physics experiments in which a ball on a pool table or a puck on an air hockey table collides with another ball or puck or with the wall (Fig. 4–1). Newton's laws are used to describe the motion of such objects, and we can accurately predict where they go and how momentum and kinetic energy are exchanged from one object to another. The kinematics of such experiments involves keeping track of the **position vector** of each object, $\vec{x}_A$, $\vec{x}_B$, . . . , and the **velocity vector** of each object, $\vec{V}_A$, $\vec{V}_B$, . . . , as functions of time (Fig. 4–2). When this method is applied to a flowing fluid, we call it the **Lagrangian description** of fluid motion after the Italian mathematician Joseph Louis Lagrange (1736–1813). Lagrangian analysis is analogous to the **system analysis** that you learned in your thermodynamics class; namely, we follow a mass of fixed identity

As you can imagine, this method of describing motion is much more difficult for fluids than for billiard balls! First of all we cannot easily define and identify particles of fluid as they move around. Secondly, a fluid is a **continuum** (from a macroscopic point of view), so interactions between parcels of fluid are not as easy to describe as are interactions between distinct objects like billiard balls or air hockey pucks. Furthermore, the fluid parcels continually *deform* as they move in the flow.

From a *microscopic* point of view, a fluid is composed of *billions* of molecules that are continuously banging into one another, somewhat like billiard balls; but the task of following even a subset of these molecules is quite difficult, even for our fastest and largest computers. Nevertheless, there are many practical applications of the Lagrangian description, such as the tracking of passive scalars in a flow, rarefied gas dynamics calculations concerning reentry of a spaceship into the earth's atmosphere, and the development of flow measurement systems based on particle imaging (as discussed in Section 4–2).

A more common method of describing fluid flow is the **Eulerian description** of fluid motion, named after the Swiss mathematician Leonhard Euler (1707–1783). In the Eulerian description of fluid flow, a finite volume called a **flow domain** or **control volume** is defined, through which fluid flows in and out. We do not need to keep track of the position and velocity of a mass of fluid particles of fixed identity. Instead, we define **field variables,** functions of space and time, within the control volume. For example, the **pressure field** is a **scalar field variable;** for general unsteady three-dimensional fluid flow in Cartesian coordinates,

Pressure field: $P = P(x, y, z, t)$ **(4–1)**

We define the **velocity field** as a **vector field variable** in similar fashion,

Velocity field: $\vec{V} = \vec{V}(x, y, z, t)$ **(4–2)**

Likewise, the **acceleration field** is also a vector field variable,

Acceleration field: $\vec{a} = \vec{a}(x, y, z, t)$ **(4–3)**

Control volume

$P(x, y, z, t)$

(x, y, z) $\vec{V}(x, y, z, t)$

Collectively, these (and other) field variables define the **flow field.** The velocity field of Eq. 4–2 can be expanded in Cartesian coordinates (x, y, z), $(\vec{i}, \vec{j}, \vec{k})$ as

$$\vec{V} = (u, v, w) = u(x, y, z, t)\vec{i} + v(x, y, z, t)\vec{j} + w(x, y, z, t)\vec{k} \qquad \textbf{(4–4)}$$

A similar expansion can be performed for the acceleration field of Eq. 4–3. In the Eulerian description, all such field variables are defined at any location (x, y, z) in the control volume and at any instant in time t (Fig. 4–3). In the Eulerian description we don't really care what happens to individual fluid particles; rather we are concerned with the pressure, velocity, acceleration, etc., of whichever fluid particle happens to be at the location of interest at the time of interest.

The difference between these two descriptions is made clearer by imagining a person standing beside a river, measuring its properties. In the Lagrangian approach, he throws in a probe that moves downstream with the water. In the Eulerian approach, he anchors the probe at a fixed location in the water.

While there are many occasions in which the Lagrangian description is useful, the Eulerian description is often more convenient for fluid mechanics applications. Furthermore, experimental measurements are generally more suited to the Eulerian description. In a wind tunnel, for example, velocity or pressure probes are usually placed at a fixed location in the flow, measuring $\vec{V}(x, y, z, t)$ or $P(x, y, z, t)$. However, whereas the equations of motion in the Lagrangian description following individual fluid particles are well known (e.g., Newton's second law), the equations of motion of fluid flow are not so readily apparent in the Eulerian description and must be carefully derived.
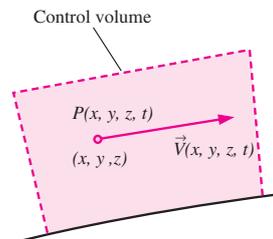
EXAMPLE 4–1   **A Steady Two-Dimensional Velocity Field**

A steady, incompressible, two-dimensional velocity field is given by

$$\vec{V} = (u, v) = (0.5 + 0.8x)\vec{i} + (1.5 - 0.8y)\vec{j} \qquad \textbf{(1)}$$

where the x- and y-coordinates are in meters and the magnitude of velocity is in m/s. A **stagnation point** is defined as *a point in the flow field where the velocity is identically zero.* (*a*) Determine if there are any stagnation points in this flow field and, if so, where? (*b*) Sketch velocity vectors at several locations in the domain between $x = -2$ m to 2 m and $y = 0$ m to 5 m; qualitatively describe the flow field.

SOLUTION   For the given velocity field, the location(s) of stagnation point(s) are to be determined. Several velocity vectors are to be sketched and the velocity field is to be described.
Assumptions   **1** The flow is steady and incompressible. **2** The flow is two-dimensional, implying no z-component of velocity and no variation of u or v with z.
Analysis   (*a*) Since $\vec{V}$ is a vector, *all* its components must equal zero in order for $\vec{V}$ itself to be zero. Using Eq. 4–4 and setting Eq. 1 equal to zero,

Stagnation point:
$$u = 0.5 + 0.8x = 0 \quad \rightarrow \quad x = -0.625 \text{ m}$$
$$v = 1.5 - 0.8y = 0 \quad \rightarrow \quad y = 1.875 \text{ m}$$

Yes. There is one stagnation point located at **$x = -0.625$ m, $y = 1.875$ m.**
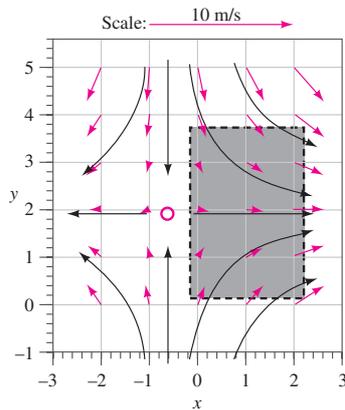
FIGURE 4–4
Velocity vectors for the velocity field of Example 4–1. The scale is shown by the top arrow, and the solid black curves represent the approximate shapes of some streamlines, based on the calculated velocity vectors. The stagnation point is indicated by the blue circle. The shaded region represents a portion of the flow field that can approximate flow into an inlet (Fig. 4–5).
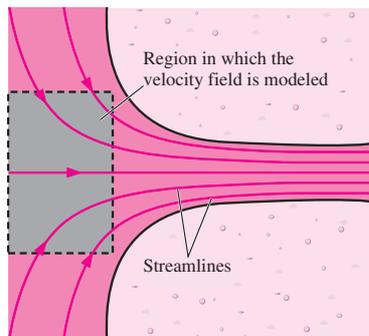
FIGURE 4–5
Flow field near the bell mouth inlet of a hydroelectric dam; a portion of the velocity field of Example 4–1 may be used as a first-order approximation of this physical flow field. The shaded region corresponds to that of Fig. 4–4.

(*b*) The *x*- and *y*-components of velocity are calculated from Eq. 1 for several (*x*, *y*) locations in the specified range. For example, at the point (*x* = 2 m, *y* = 3 m), *u* = 2.10 m/s and *v* = −0.900 m/s. The magnitude of velocity (the *speed*) at that point is 2.28 m/s. At this and at an array of other locations, the velocity vector is constructed from its two components, the results of which are shown in Fig. 4–4. The flow can be described as stagnation point flow in which flow enters from the top and bottom and spreads out to the right and left about a horizontal line of symmetry at *y* = 1.875 m. The stagnation point of part (*a*) is indicated by the blue circle in Fig. 4–4.

If we look only at the shaded portion of Fig. 4–4, this flow field models a converging, accelerating flow from the left to the right. Such a flow might be encountered, for example, near the submerged bell mouth inlet of a hydro-electric dam (Fig. 4–5). The useful portion of the given velocity field may be thought of as a first-order approximation of the shaded portion of the physical flow field of Fig. 4–5.

Discussion   It can be verified from the material in Chap. 9 that this flow field is physically valid because it satisfies the differential equation for conservation of mass.

Acceleration Field

As you should recall from your study of thermodynamics, the fundamental conservation laws (such as conservation of mass and the first law of thermodynamics) are expressed for a *system* of fixed identity (also called a *closed system*). In cases where analysis of a *control volume* (also called an *open system*) is more convenient than system analysis, it is necessary to rewrite these fundamental laws into forms applicable to the control volume. The same principle applies here. In fact, there is a direct analogy between systems versus control volumes in thermodynamics and Lagrangian versus Eulerian descriptions in fluid dynamics. The equations of motion for fluid flow (such as Newton's second law) are written for an object of fixed identity, taken here as a small fluid parcel, which we call a **fluid particle** or **material particle.** If we were to follow a particular fluid particle as it moves around in the flow, we would be employing the Lagrangian description, and the equations of motion would be directly applicable. For example, we would define the particle's location in space in terms of a **material position vector** $(x_{\text{particle}}(t), y_{\text{particle}}(t), z_{\text{particle}}(t))$. However, some mathematical manipulation is then necessary to convert the equations of motion into forms applicable to the Eulerian description.

Consider, for example, Newton's second law applied to our fluid particle,

Newton's second law: $\vec{F}_{\text{particle}} = m_{\text{particle}}\vec{a}_{\text{particle}}$ **(4–5)**

where $\vec{F}_{\text{particle}}$ is the net force acting on the fluid particle, m_{particle} is its mass, and $\vec{a}_{\text{particle}}$ is its acceleration (Fig. 4–6). By definition, the acceleration of the fluid particle is the time derivative of the particle's velocity,

Acceleration of a fluid particle: $\vec{a}_{\text{particle}} = \dfrac{d\vec{V}_{\text{particle}}}{dt}$ **(4–6)**

However, at any instant in time *t*, the velocity of the particle is the same as the local value of the velocity *field* at the location $(x_{\text{particle}}(t), y_{\text{particle}}(t),$

$z_{particle}(t))$ of the particle, since the fluid particle moves with the fluid by definition. In other words, $\vec{V}_{particle}(t) \equiv \vec{V}(x_{particle}(t), y_{particle}(t), z_{particle}(t), t)$. To take the time derivative in Eq. 4–6, we must therefore use the *chain rule*, since the dependent variable $(\vec{V})$ is a function of *four* independent variables $(x_{particle}, y_{particle}, z_{particle},$ and $t)$,

$$\vec{a}_{particle} = \frac{d\vec{V}_{particle}}{dt} = \frac{d\vec{V}}{dt} = \frac{d\vec{V}(x_{particle}, y_{particle}, z_{particle}, t)}{dt}$$

$$= \frac{\partial \vec{V}}{\partial t}\frac{dt}{dt} + \frac{\partial \vec{V}}{\partial x_{particle}}\frac{dx_{particle}}{dt} + \frac{\partial \vec{V}}{\partial y_{particle}}\frac{dy_{particle}}{dt} + \frac{\partial \vec{V}}{\partial z_{particle}}\frac{dz_{particle}}{dt}$$

(4–7)

In Eq. 4–7, ∂ is the **partial derivative operator** and d is the **total derivative operator.** Consider the second term on the right-hand side of Eq. 4–7. Since the acceleration is defined as that *following a fluid particle* (Lagrangian description), the rate of change of the particle's x-position with respect to time is $dx_{particle}/dt = u$ (Fig. 4–7), where u is the x-component of the velocity vector defined by Eq. 4–4. Similarly, $dy_{particle}/dt = v$ and $dz_{particle}/dt = w$. Furthermore, at any instant in time under consideration, the material position vector $(x_{particle}, y_{particle}, z_{particle})$ of the fluid particle in the Lagrangian frame is equal to the position vector (x, y, z) in the Eulerian frame. Equation 4–7 thus becomes

$$\vec{a}_{particle}(x, y, z, t) = \frac{d\vec{V}}{dt} = \frac{\partial \vec{V}}{\partial t} + u\frac{\partial \vec{V}}{\partial x} + v\frac{\partial \vec{V}}{\partial y} + w\frac{\partial \vec{V}}{\partial z}$$

(4–8)

where we have also used the (obvious) fact that $dt/dt = 1$. Finally, at any instant in time t, the acceleration field of Eq. 4–3 must equal the acceleration of the fluid particle that happens to occupy the location (x, y, z) at that time t, since the fluid particle is by definition accelerating with the fluid flow. Hence, *we may replace $\vec{a}_{particle}$ with $\vec{a}(x, y, z, t)$ in Eqs. 4–7 and 4–8 to transform from the Lagrangian to the Eulerian frame of reference*. In vector form, Eq. 4–8 can be written as

Acceleration of a fluid particle expressed as a field variable:

$$\vec{a}(x, y, z, t) = \frac{d\vec{V}}{dt} = \frac{\partial \vec{V}}{\partial t} + (\vec{V} \cdot \vec{\nabla})\vec{V}$$

(4–9)

where $\vec{\nabla}$ is the **gradient operator** or **del operator,** a vector operator that is defined in Cartesian coordinates as

Gradient or del operator:
$$\vec{\nabla} = \left(\frac{\partial}{\partial x}, \frac{\partial}{\partial y}, \frac{\partial}{\partial z}\right) = \vec{i}\frac{\partial}{\partial x} + \vec{j}\frac{\partial}{\partial y} + \vec{k}\frac{\partial}{\partial z}$$
(4–10)

In Cartesian coordinates then, the components of the acceleration vector are

$$a_x = \frac{\partial u}{\partial t} + u\frac{\partial u}{\partial x} + v\frac{\partial u}{\partial y} + w\frac{\partial u}{\partial z}$$

Cartesian coordinates:
$$a_y = \frac{\partial v}{\partial t} + u\frac{\partial v}{\partial x} + v\frac{\partial v}{\partial y} + w\frac{\partial v}{\partial z}$$
(4–11)

$$a_z = \frac{\partial w}{\partial t} + u\frac{\partial w}{\partial x} + v\frac{\partial w}{\partial y} + w\frac{\partial w}{\partial z}$$
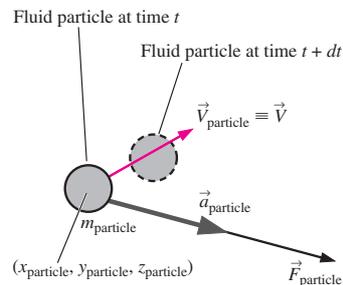
FIGURE 4–6

Newton's second law applied to a fluid particle; the acceleration vector (gray arrow) is in the same direction as the force vector (black arrow), but the velocity vector (blue arrow) may act in a different direction.
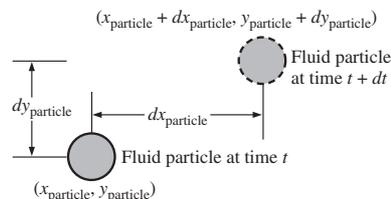
FIGURE 4–7

When following a fluid particle, the x-component of velocity, u, is defined as $dx_{particle}/dt$. Similarly, $v = dy_{particle}/dt$ and $w = dz_{particle}/dt$. Movement is shown here only in two dimensions for simplicity.
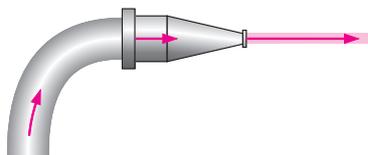
FIGURE 4–8
Flow of water through the nozzle of a garden hose illustrates that fluid particles may accelerate, even in a steady flow. In this example, the exit speed of the water is much higher than the water speed in the hose, implying that fluid particles have accelerated even though the flow is steady.

The first term on the right-hand side of Eq. 4–9, $\partial \vec{V}/\partial t$, is called the **local acceleration** and is nonzero only for unsteady flows. The second term, $(\vec{V} \cdot \vec{\nabla})\vec{V}$, is called the **advective acceleration** (sometimes the **convective acceleration**); *this term can be nonzero even for steady flows*. It accounts for the effect of the fluid particle moving (advecting or convecting) to a new location in the flow, where the velocity field is different. For example, consider steady flow of water through a garden hose nozzle (Fig. 4–8). We define *steady* in the Eulerian frame of reference to be when properties at any point in the flow field do not change with respect to time. Since the velocity at the exit of the nozzle is larger than that at the nozzle entrance, fluid particles clearly accelerate, even though the flow is steady. The acceleration is nonzero because of the advective acceleration terms in Eq. 4–9. Note that while the flow is steady from the point of view of a fixed observer in the Eulerian reference frame, it is *not* steady from the Lagrangian reference frame moving with a fluid particle that enters the nozzle and accelerates as it passes through the nozzle.

EXAMPLE 4–2   **Acceleration of a Fluid Particle through a Nozzle**

Nadeen is washing her car, using a nozzle similar to the one sketched in Fig. 4–8. The nozzle is 3.90 in (0.325 ft) long, with an inlet diameter of 0.420 in (0.0350 ft) and an outlet diameter of 0.182 in (see Fig. 4–9). The volume flow rate through the garden hose (and through the nozzle) is $\dot{V}$ = 0.841 gal/min (0.00187 ft³/s), and the flow is steady. Estimate the magnitude of the acceleration of a fluid particle moving down the centerline of the nozzle.

SOLUTION   The acceleration following a fluid particle down the center of a nozzle is to be estimated.
Assumptions   **1** The flow is steady and incompressible. **2** The *x*-direction is taken along the centerline of the nozzle. **3** By symmetry, $v = w = 0$ along the centerline, but *u* increases through the nozzle.
Analysis   The flow is steady, so you may be tempted to say that the acceleration is zero. However, even though the local acceleration $\partial \vec{V}/\partial t$ is identically zero for this steady flow field, the advective acceleration $(\vec{V} \cdot \vec{\nabla})\vec{V}$ is *not* zero. We first calculate the average *x*-component of velocity at the inlet and outlet of the nozzle by dividing volume flow rate by cross-sectional area:

Inlet speed:

$$u_{\text{inlet}} \cong \frac{\dot{V}}{A_{\text{inlet}}} = \frac{4\dot{V}}{\pi D_{\text{inlet}}^2} = \frac{4(0.00187 \text{ ft}^3/\text{s})}{\pi(0.0350 \text{ ft})^2} = 1.95 \text{ ft/s}$$

Similarly, the average outlet speed is u_{outlet} = 10.4 ft/s. We now calculate the acceleration two ways, with equivalent results. First, a simple average value of acceleration in the *x*-direction is calculated based on the change in speed divided by an estimate of the **residence time** of a fluid particle in the nozzle, $\Delta t = \Delta x/u_{\text{avg}}$ (Fig. 4–10). By the fundamental definition of acceleration as the rate of change of velocity,

Method A: $a_x \cong \dfrac{\Delta u}{\Delta t} = \dfrac{u_{\text{outlet}} - u_{\text{inlet}}}{\Delta x/u_{\text{avg}}} = \dfrac{u_{\text{outlet}} - u_{\text{inlet}}}{2\,\Delta x/(u_{\text{outlet}} + u_{\text{inlet}})} = \dfrac{u_{\text{outlet}}^2 - u_{\text{inlet}}^2}{2\,\Delta x}$
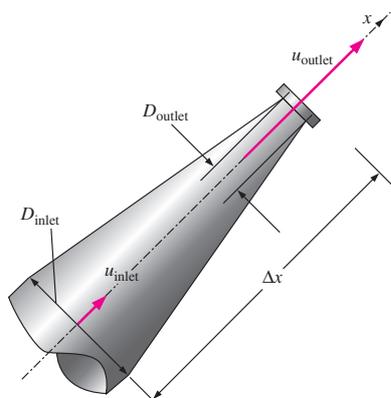
FIGURE 4–9
Flow of water through the nozzle of Example 4–2.

The second method uses the equation for acceleration field components in Cartesian coordinates, Eq. 4–11,

Method B: $\quad a_x = \underbrace{\frac{\partial u}{\partial t}}_{0} + u\frac{\partial u}{\partial x} + \underbrace{v\frac{\partial u}{\partial y}}_{0} + \underbrace{w\frac{\partial u}{\partial z}}_{0} \cong u_{\text{avg}}\frac{\Delta u}{\Delta x}$

$\quad\quad\quad\quad\quad$ Steady $\quad\quad$ $v = 0$ along centerline $\quad$ $w = 0$ along centerline

Here we see that only one advective term is nonzero. We approximate the average speed through the nozzle as the average of the inlet and outlet speeds, and we use a **first-order finite difference approximation** (Fig. 4–11) for the average value of derivative $\partial u/\partial x$ through the centerline of the nozzle:

$$a_x \cong \frac{u_{\text{outlet}} + u_{\text{inlet}}}{2}\frac{u_{\text{outlet}} - u_{\text{inlet}}}{\Delta x} = \frac{u_{\text{outlet}}^2 - u_{\text{inlet}}^2}{2\,\Delta x}$$

The result of method B is identical to that of method A. Substitution of the given values yields

Axial acceleration:

$$a_x \cong \frac{u_{\text{outlet}}^2 - u_{\text{inlet}}^2}{2\,\Delta x} = \frac{(10.4\text{ ft/s})^2 - (1.95\text{ ft/s})^2}{2(0.325\text{ ft})} = \mathbf{160\text{ ft/s}^2}$$

Discussion Fluid particles are accelerated through the nozzle at nearly five times the acceleration of gravity (almost five *g*'s)! This simple example clearly illustrates that the acceleration of a fluid particle can be nonzero, even in steady flow. Note that the acceleration is actually a **point function,** whereas we have estimated a simple average acceleration through the entire nozzle.
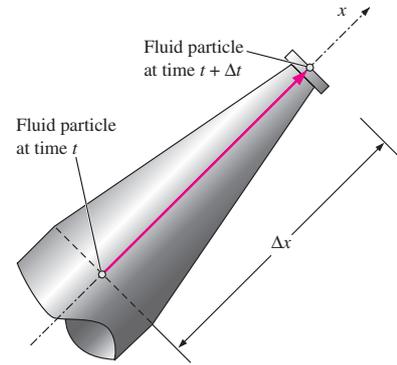
FIGURE 4–10
Residence time Δt is defined as the time it takes for a fluid particle to travel through the nozzle from inlet to outlet (distance Δx).
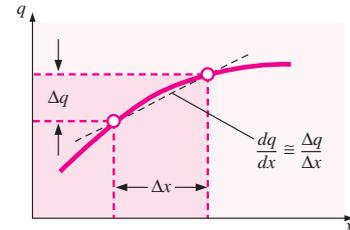
FIGURE 4–11
A *first-order finite difference approximation* for derivative dq/dx is simply the change in dependent variable (q) divided by the change in independent variable (x).

Material Derivative

The total derivative operator d/dt in Eq. 4–9 is given a special name, the **material derivative;** some authors also assign to it a special notation, D/Dt, in order to emphasize that it is formed by *following a fluid particle as it moves through the flow field* (Fig. 4–12). Other names for the material derivative include **total**, **particle**, **Lagrangian**, **Eulerian**, and **substantial derivative**.

Material derivative: $\quad\quad \dfrac{D}{Dt} = \dfrac{d}{dt} = \dfrac{\partial}{\partial t} + (\vec{V}\cdot\vec{\nabla})$ $\quad\quad\quad$ **(4–12)**

When we apply the material derivative of Eq. 4–12 to the velocity field, the result is the acceleration field as expressed by Eq. 4–9, which is thus sometimes called the **material acceleration.**

Material acceleration: $\quad \vec{a}(x, y, z, t) = \dfrac{D\vec{V}}{Dt} = \dfrac{d\vec{V}}{dt} = \dfrac{\partial\vec{V}}{\partial t} + (\vec{V}\cdot\vec{\nabla})\vec{V}$ $\quad$ **(4–13)**

Equation 4–12 can also be applied to other fluid properties besides velocity, both scalars and vectors. For example, the material derivative of pressure can be written as

Material derivative of pressure: $\quad \dfrac{DP}{Dt} = \dfrac{dP}{dt} = \dfrac{\partial P}{\partial t} + (\vec{V}\cdot\vec{\nabla})P$ $\quad$ **(4–14)**
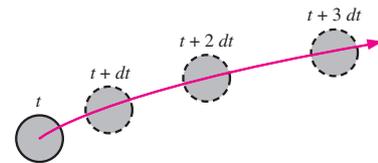
FIGURE 4–12
The material derivative *D/Dt* is defined by following a fluid particle as it moves throughout the flow field. In this illustration, the fluid particle is accelerating to the right as it moves up and to the right.

128
FLUID MECHANICS

$$\underbrace{\frac{D}{Dt}}_{\substack{\text{Material} \\ \text{derivative}}} = \underbrace{\frac{\partial}{\partial t}}_{\text{Local}} + \underbrace{(\vec{V} \cdot \vec{\nabla})}_{\text{Advective}}$$

FIGURE 4–13
The material derivative *D/Dt* is composed of a *local* or *unsteady* part and a *convective* or *advective* part.

Equation 4–14 represents the time rate of change of pressure following a fluid particle as it moves through the flow and contains both local (unsteady) and advective components (Fig. 4–13).

EXAMPLE 4–3   Material Acceleration of a Steady Velocity Field

Consider the steady, incompressible, two-dimensional velocity field of Example 4–1. (*a*) Calculate the material acceleration at the point ($x = 2$ m, $y = 3$ m). (*b*) Sketch the material acceleration vectors at the same array of *x*- and *y*-values as in Example 4–1.

SOLUTION   For the given velocity field, the material acceleration vector is to be calculated at a particular point and plotted at an array of locations in the flow field.
Assumptions **1** The flow is steady and incompressible. **2** The flow is two-dimensional, implying no *z*-component of velocity and no variation of *u* or *v* with *z*.
Analysis   (*a*) Using the velocity field of Eq. 1 of Example 4–1 and the equation for material acceleration components in Cartesian coordinates (Eq. 4–11), we write expressions for the two nonzero components of the acceleration vector:

$$a_x = \frac{\partial u}{\partial t} + u\frac{\partial u}{\partial x} + v\frac{\partial u}{\partial y} + w\frac{\partial u}{\partial z}$$
$$= 0 + (0.5 + 0.8x)(0.8) + (15 - 0.8y)(0) + 0 = (0.4 + 0.64x) \text{ m/s}^2$$

and

$$a_y = \frac{\partial v}{\partial t} + u\frac{\partial v}{\partial x} + v\frac{\partial v}{\partial y} + w\frac{\partial v}{\partial z}$$
$$= 0 + (0.5 + 0.8x)(0) + (1.5 - 0.8y)(-0.8) + 0 = (-1.2 + 0.64y) \text{ m/s}^2$$

At the point ($x = 2$ m, $y = 3$ m), **$a_x = 1.68$ m/s^2 and $a_y = 0.720$ m/s^2.**
(*b*) The equations in part (*a*) are applied to an array of *x*- and *y*-values in the flow domain within the given limits, and the acceleration vectors are plotted in Fig. 4–14.
Discussion   The acceleration field is nonzero, even though the flow is *steady*. Above the stagnation point (above $y = 1.875$ m), the acceleration vectors plotted in Fig. 4–14 point upward, increasing in magnitude away from the stagnation point. To the right of the stagnation point (to the right of $x = -0.625$ m), the acceleration vectors point to the right, again increasing in magnitude away from the stagnation point. This agrees qualitatively with the velocity vectors of Fig. 4–4 and the streamlines sketched in Fig. 4–14; namely, in the upper-right portion of the flow field, fluid particles are accelerated in the upper-right direction and therefore veer in the counterclockwise direction due to **centripetal acceleration** toward the upper right. The flow below $y = 1.875$ m is a mirror image of the flow above this symmetry line, and flow to the left of $x = -0.625$ m is a mirror image of the flow to the right of this symmetry line.
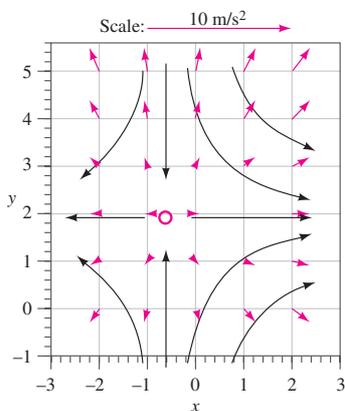
FIGURE 4–14
Acceleration vectors for the velocity field of Examples 4–1 and 4–3. The scale is shown by the top arrow, and the solid black curves represent the approximate shapes of some streamlines, based on the calculated velocity vectors (see Fig. 4–4). The stagnation point is indicated by the blue circle.

4–2 ▪ FUNDAMENTALS OF FLOW VISUALIZATION

While quantitative study of fluid dynamics requires advanced mathematics, much can be learned from **flow visualization**—the visual examination of flow field features. Flow visualization is useful not only in physical experiments (Fig. 4–15), but in *numerical* solutions as well [**computational fluid dynamics (CFD)**]. In fact, the very first thing an engineer using CFD does after obtaining a numerical solution is simulate some form of flow visualization, so that he or she can see the "whole picture" rather than merely a list of numbers and quantitative data. Why? Because the human mind is designed to rapidly process an incredible amount of visual information; as they say, a picture is worth a thousand words. There are many types of flow patterns that can be visualized, both physically (experimentally) and/or computationally.
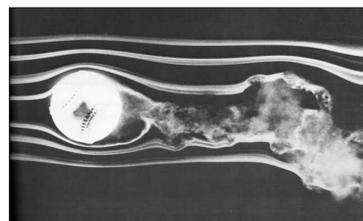
FIGURE 4–15
Spinning baseball.
The late F. N. M. Brown devoted many years to developing and using smoke visualization in wind tunnels at the University of Notre Dame. Here the flow speed is about 77 ft/s and the ball is rotated at 630 rpm.
Photograph courtesy of T. J. Mueller.

Streamlines and Streamtubes

> A **streamline** is a curve that is everywhere tangent to the instantaneous local velocity vector.

Streamlines are useful as indicators of the instantaneous direction of fluid motion throughout the flow field. For example, regions of recirculating flow and separation of a fluid off of a solid wall are easily identified by the streamline pattern. Streamlines cannot be directly observed experimentally except in steady flow fields, in which they are coincident with pathlines and streaklines, to be discussed next. Mathematically, however, we can write a simple expression for a streamline based on its definition.

Consider an infinitesimal arc length $d\vec{r} = dx\vec{i} + dy\vec{j} + dz\vec{k}$ along a streamline; $d\vec{r}$ must be parallel to the local velocity vector $\vec{V} = u\vec{i} + v\vec{j} + w\vec{k}$ by definition of the streamline. By simple geometric arguments using similar triangles, we know that the components of $d\vec{r}$ must be proportional to those of $\vec{V}$ (Fig. 4–16). Hence,

Equation for a streamline:
$$\frac{dr}{V} = \frac{dx}{u} = \frac{dy}{v} = \frac{dz}{w}$$
(4–15)

where dr is the magnitude of $d\vec{r}$ and V is the speed, the magnitude of $\vec{V}$. Equation 4–15 is illustrated in two dimensions for simplicity in Fig. 4–16. For a known velocity field, we can integrate Eq. 4–15 to obtain equations for the streamlines. In two dimensions, (x, y), (u, v), the following differential equation is obtained:

Streamline in the xy-plane:
$$\left(\frac{dy}{dx}\right)_{\text{along a streamline}} = \frac{v}{u}$$
(4–16)

In some simple cases, Eq. 4–16 may be solvable analytically; in the general case, it must be solved numerically. In either case, an arbitrary constant of integration appears, and the *family* of curves that satisfy Eq. 4–16 represents streamlines of the flow field.
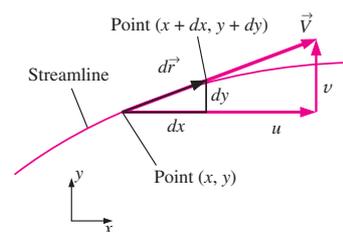
FIGURE 4–16
For two-dimensional flow in the *xy*-plane, arc length $d\vec{r} = (dx, dy)$ along a *streamline* is everywhere tangent to the local instantaneous velocity vector $\vec{V} = (u, v)$.

**130
FLUID MECHANICS**
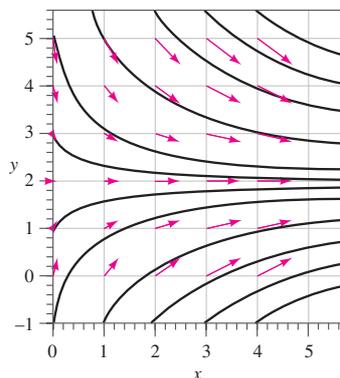
FIGURE 4–17
Streamlines (solid black curves) for
the velocity field of Example 4–4;
velocity vectors of Fig. 4–4 (blue
arrows) are superimposed for
comparison.

**EXAMPLE 4–4   Streamlines in the *xy*-Plane—An Analytical
Solution**

For the steady, incompressible, two-dimensional velocity field of Example
4–1, plot several streamlines in the right half of the flow ($x > 0$) and com-
pare to the velocity vectors plotted in Fig. 4–4.

SOLUTION An analytical expression for streamlines is to be generated and
plotted in the upper-right quadrant.
Assumptions **1** The flow is steady and incompressible. **2** The flow is two-
dimensional, implying no *z*-component of velocity and no variation of *u* or *v*
with *z*.
Analysis Equation 4–16 is applicable here; thus, along a streamline,

$$\frac{dy}{dx} = \frac{1.5 - 0.8y}{0.5 + 0.8x}$$

We solve this differential equation by separation of variables:

$$\frac{dy}{1.5 - 0.8y} = \frac{dx}{0.5 + 0.8x} \quad \rightarrow \quad \int \frac{dy}{1.5 - 0.8y} = \int \frac{dx}{0.5 + 0.8x}$$

After some algebra (which we leave to the reader), we solve for *y* as a func-
tion of *x* along a streamline,

$$y = \frac{C}{0.8(0.5 + 0.8x)} + 1.875$$

where *C* is a constant of integration that can be set to various values in order
to plot the streamlines. Several streamlines of the given flow field are shown
in Fig. 4–17.
Discussion The velocity vectors of Fig. 4–4 are superimposed on the
streamlines of Fig. 4–17; the agreement is excellent in the sense that the
velocity vectors point everywhere tangent to the streamlines. Note that speed
cannot be determined directly from the streamlines alone.

A **streamtube** consists of a bundle of streamlines (Fig. 4–18), much like
a communications cable consists of a bundle of fiber-optic cables. Since
streamlines are everywhere parallel to the local velocity, fluid cannot cross a
streamline by definition. By extension, *fluid within a streamtube must
remain there and cannot cross the boundary of the streamtube*. You must
keep in mind that both streamlines and streamtubes are instantaneous quan-
tities, defined at a particular instant in time according to the velocity field at
that instant. In an *unsteady* flow, the streamline pattern may change signifi-
cantly with time. Nevertheless, at any instant in time, the mass flow rate
passing through any cross-sectional slice of a given streamtube must remain
the same. For example, in a converging portion of an incompressible flow
field, the diameter of the streamtube must decrease as the velocity increases
so as to conserve mass (Fig. 4–19*a*). Likewise, the streamtube diameter
increases in diverging portions of the incompressible flow (Fig. 4–19*b*).

FIGURE 4–18
A *streamtube* consists of a bundle of
individual streamlines.

Pathlines

A **pathline** is the actual path traveled by an individual fluid particle over some
time period.
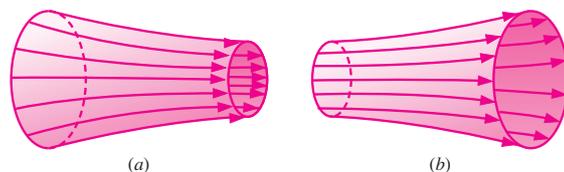
FIGURE 4–19
In an incompressible flow field, a streamtube (*a*) decreases in diameter as the flow accelerates or converges and (*b*) increases in diameter as the flow decelerates or diverges.

Pathlines are the easiest of the flow patterns to understand. A pathline is a Lagrangian concept in that we simply follow the path of an individual fluid particle as it moves around in the flow field (Fig. 4–20). Thus, a pathline is the same as the fluid particle's material position vector ($x_{\text{particle}}(t)$, $y_{\text{particle}}(t)$, $z_{\text{particle}}(t)$), discussed in Section 4–1, traced out over some finite time interval. In a physical experiment, you can imagine a tracer fluid particle that is marked somehow—either by color or brightness—such that it is easily distinguishable from surrounding fluid particles. Now imagine a camera with the shutter open for a certain time period, $t_{\text{start}} < t < t_{\text{end}}$, in which the particle's path is recorded; the resulting curve is called a pathline. An intriguing example is shown in Fig. 4–21 for the case of waves moving along the surface of water in a tank. Neutrally buoyant white **tracer particles** are suspended in the water, and a time-exposure photograph is taken for one complete wave period. The result is pathlines that are elliptical in shape, showing that fluid particles bob up and down and forward and backward, but return to their original position upon completion of one wave period; there is no net forward motion. You may have experienced something similar while bobbing up and down on ocean waves.
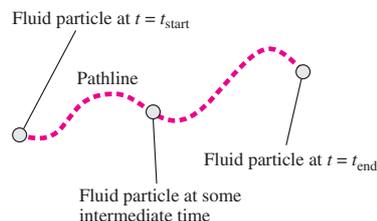
FIGURE 4–20
A *pathline* is formed by following the actual path of a fluid particle.
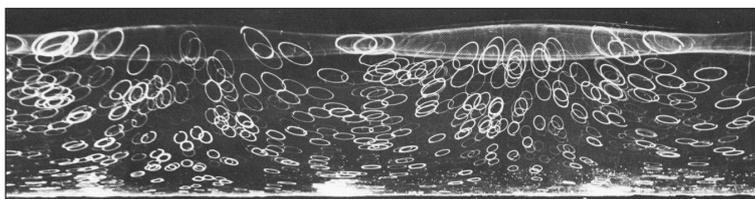
FIGURE 4–21
Pathlines produced by white tracer particles suspended in water and captured by time-exposure photography; as waves pass horizontally, each particle moves in an elliptical path during one wave period.
Wallet, A. & Ruellan, F. 1950, La Houille Blanche *5:483–489. Used by permission.*

A modern experimental technique called **particle image velocimetry (PIV)** utilizes particle pathlines to measure the velocity field over an entire plane in a flow (Adrian, 1991). (Recent advances also extend the technique to three dimensions.) In PIV, tiny tracer particles are suspended in the fluid, much like in Fig. 4–21. However, the flow is illuminated by two flashes of light (usually from a laser as in Fig. 4–22) to produce two bright spots on the film or photosensor for each moving particle. Then, both the magnitude and direction of the velocity vector at each particle location can be inferred, assuming that the tracer particles are small enough that they move with the fluid. Modern digital photography and fast computers have enabled PIV to be performed rapidly enough so that *unsteady* features of a flow field can also be measured. PIV is discussed in more detail in Chap. 8.

FIGURE 4–22
PIV applied to a model car in a wind tunnel.
*Courtesy Dantec Dynamics, Inc.
Used by permission.*
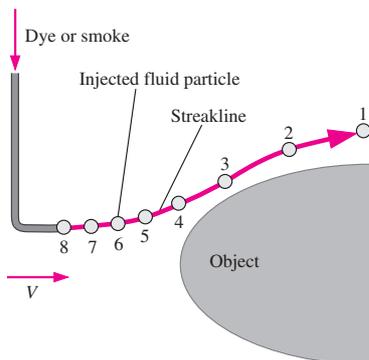
FIGURE 4–23

A *streakline* is formed by continuous introduction of dye or smoke from a point in the flow. Labeled tracer particles (1 through 8) were introduced sequentially.

Pathlines can also be calculated numerically for a known velocity field. Specifically, the location of the tracer particle is integrated over time from some starting location $\vec{x}_{start}$ and starting time t_{start} to some later time t.

Tracer particle location at time t:
$$\vec{x} = \vec{x}_{start} + \int_{t_{start}}^{t} \vec{V}\, dt \qquad \text{(4–17)}$$

When Eq. 4–17 is calculated for t between t_{start} and t_{end}, a plot of $\vec{x}(t)$ is the pathline of the fluid particle during that time interval, as illustrated in Fig. 4–20. For some simple flow fields, Eq. 4–17 can be integrated analytically. For more complex flows, we must perform a numerical integration.

If the velocity field is steady, individual fluid particles will follow streamlines. Thus, *for steady flow, pathlines are identical to streamlines*.

Streaklines

A **streakline** is the locus of fluid particles that have passed sequentially through a prescribed point in the flow.

Streaklines are the most common flow pattern generated in a physical experiment. If you insert a small tube into a flow and introduce a continuous stream of tracer fluid (dye in a water flow or smoke in an airflow), the observed pattern is a streakline. Figure 4–23 shows a tracer being injected into a free-stream flow containing an object, such as the nose of a wing. The circles represent individual injected tracer fluid particles, released at a uniform time interval. As the particles are forced out of the way by the object, they accelerate around the shoulder of the object, as indicated by the increased distance between individual tracer particles in that region. The streakline is formed by connecting all the circles into a smooth curve. In physical experiments in a wind or water tunnel, the smoke or dye is injected *continuously*, not as individual particles, and the resulting flow pattern is by definition a streakline. In Fig. 4–23, tracer particle 1 was released at an earlier time than tracer particle 2, and so on. The location of an individual tracer particle is determined by the surrounding velocity field from the moment of its injection into the flow until the present time. If the flow is unsteady, the surrounding velocity field changes, and we cannot expect the resulting streakline to resemble a streamline or pathline at any given instant in time. However, *if the flow is steady, streamlines, pathlines, and streaklines are identical* (Fig. 4–24).

Streaklines are often confused with streamlines or pathlines. While the three flow patterns are identical in steady flow, they can be quite different in unsteady flow. The main difference is that a streamline represents an *instantaneous* flow pattern at a given instant in time, while a streakline and a pathline are flow patterns that have some *age* and thus a *time history* associated with them. A streakline is an instantaneous snapshot of a *time-integrated* flow pattern. A pathline, on the other hand, is the *time-exposed* flow path of an individual particle over some time period.

The time-integrative property of streaklines is vividly illustrated in an experiment by Cimbala et al. (1988), reproduced here as Fig. 4–25. The authors used a **smoke wire** for flow visualization in a wind tunnel. In operation, the smoke wire is a thin vertical wire that is coated with mineral oil.

FIGURE 4–24

Streaklines produced by colored fluid introduced upstream; since the flow is steady, these streaklines are the same as streamlines and pathlines.

Courtesy ONERA. Photograph by Werlé.

Cylinder

(*a*)

x/D

0   50   100   150   200   250

(*b*)
Cylinder
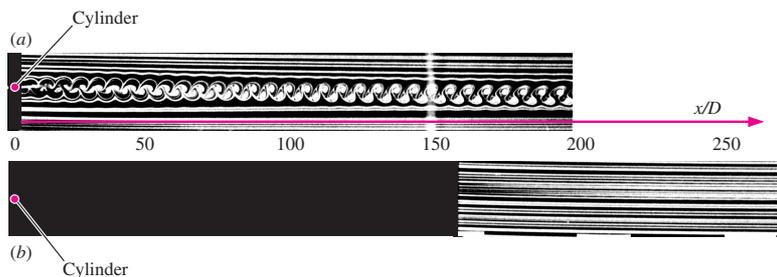
FIGURE 4–25

Smoke streaklines introduced by a smoke wire at two different locations in the wake of a circular cylinder: (*a*) smoke wire just downstream of the cylinder and (*b*) smoke wire located at *x/D* = 150. The time-integrative nature of streaklines is clearly seen by comparing the two photographs.

Photos by John M. Cimbala.

The oil breaks up into beads along the length of the wire due to surface tension effects. When an electric current heats the wire, each little bead of oil produces a streakline of smoke. In Fig. 4–25*a*, streaklines are introduced from a smoke wire located just downstream of a circular cylinder of diameter *D* aligned normal to the plane of view. (When multiple streaklines are introduced along a line, as in Fig. 4–25, we refer to this as a **rake** of streaklines.) The Reynolds number of the flow is Re = $\rho VD/\mu$ = 93. Because of unsteady **vortices** shed in an alternating pattern from the cylinder, the smoke collects into a clearly defined pattern called a **Kármán vortex street.**

From Fig. 4–25*a* alone, one may think that the shed vortices continue to exist to several hundred diameters downstream of the cylinder. However, the streakline pattern of this figure is misleading! In Fig. 4–25*b*, the smoke wire is placed 150 diameters downstream of the cylinder. The resulting streaklines are straight, indicating that the shed vortices have in reality disappeared by this downstream distance. The flow is steady and parallel at this location, and there are no more vortices; viscous diffusion has caused adjacent vortices of opposite sign to cancel each other out by around 100 cylinder diameters. The patterns of Fig. 4–25*a* near *x/D* = 150 are merely *remnants* of the vortex street that existed upstream. The streaklines of Fig. 4–25*b*, however, show the correct features of the flow at that location. The streaklines generated at *x/D* = 150 are identical to streamlines or pathlines in that region of the flow—straight, nearly horizontal lines—since the flow is steady there.

For a known velocity field, a streakline can be generated numerically, although with some difficulty. One needs to follow the paths of a continuous stream of tracer particles from the time of their injection into the flow until the present time, using Eq. 4–17. Mathematically, the location of a tracer particle is integrated over time from the time of its injection t_{inject} to the present time $t_{present}$. Equation 4–17 becomes

Integrated tracer particle location: $$\vec{x} = \vec{x}_{injection} + \int_{t_{inject}}^{t_{present}} \vec{V}\, dt$$ **(4–18)**

In a complex unsteady flow, the time integration must be performed numerically as the velocity field changes with time. When the locus of tracer particle locations at $t = t_{\text{present}}$ is connected by a smooth curve, the result is the desired streakline.
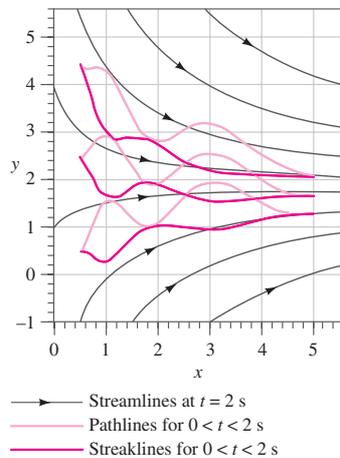
FIGURE 4–26
Streamlines, pathlines, and streaklines for the oscillating velocity field of Example 4–5. The streaklines and pathlines are wavy because of their integrated time history, but the streamlines are not wavy since they represent an instantaneous snapshot of the velocity field.

Legend:
———▶ Streamlines at $t = 2$ s
——— Pathlines for $0 < t < 2$ s
——— Streaklines for $0 < t < 2$ s

EXAMPLE 4–5   **Comparison of Flow Patterns in an Unsteady Flow**

An *unsteady*, incompressible, two-dimensional velocity field is given by

$$\vec{V} = (u, v) = (0.5 + 0.8x)\vec{i} + (1.5 + 2.5 \sin(\omega t) - 0.8y)\vec{j} \qquad (1)$$

where the angular frequency ω is equal to 2π rad/s (a physical frequency of 1 Hz). This velocity field is identical to that of Eq. 1 of Example 4–1 except for the additional periodic term in the v-component of velocity. In fact, since the period of oscillation is 1 s, when time t is any integral multiple of $\frac{1}{2}$ s ($t = 0, \frac{1}{2}, 1, \frac{3}{2}, 2, \ldots$ s), the sine term in Eq. 1 is zero and the velocity field is instantaneously identical to that of Example 4–1. Physically, we imagine flow into a large bell mouth inlet that is oscillating up and down at a frequency of 1 Hz. Consider two complete cycles of flow from $t = 0$ s to $t = 2$ s. Compare instantaneous streamlines at $t = 2$ s to pathlines and streaklines generated during the time period from $t = 0$ s to $t = 2$ s.

SOLUTION   Streamlines, pathlines, and streaklines are to be generated and compared for the given unsteady velocity field.
Assumptions   **1** The flow is incompressible. **2** The flow is two-dimensional, implying no z-component of velocity and no variation of u or v with z.
Analysis   The instantaneous streamlines at $t = 2$ s are identical to those of Fig. 4–17, and several of them are replotted in Fig. 4–26. To simulate pathlines, we use the Runge–Kutta numerical integration technique to march in time from $t = 0$ s to $t = 2$ s, tracing the path of fluid particles released at three locations: ($x = 0.5$ m, $y = 0.5$ m), ($x = 0.5$ m, $y = 2.5$ m), and ($x = 0.5$ m, $y = 4.5$ m). These pathlines are shown in Fig. 4–26, along with the streamlines. Finally, streaklines are simulated by following the paths of *many* fluid tracer particles released at the given three locations at times between $t = 0$ s and $t = 2$ s, and connecting the locus of their positions at $t = 2$ s. These streaklines are also plotted in Fig. 4–26.
Discussion   Since the flow is unsteady, the streamlines, pathlines, and streaklines are *not* coincident. In fact, they differ significantly from each other. Note that the streaklines and pathlines are wavy due to the undulating v-component of velocity. Two complete periods of oscillation have occurred between $t = 0$ s and $t = 2$ s, as verified by a careful look at the pathlines and streaklines. The streamlines have no such waviness since they have no time history; they represent an instantaneous snapshot of the velocity field at $t = 2$ s.

Timelines

A **timeline** is a set of adjacent fluid particles that were marked at the same (earlier) instant in time.

Timelines are particularly useful in situations where the uniformity of a flow (or lack thereof) is to be examined. Figure 4–27 illustrates timelines in

a channel flow between two parallel walls. Because of friction at the walls, the fluid velocity there is zero (the no-slip condition), and the top and bottom of the timeline are anchored at their starting locations. In regions of the flow away from the walls, the marked fluid particles move at the local fluid velocity, deforming the timeline. In the example of Fig. 4–27, the speed near the center of the channel is fairly uniform, but small deviations tend to amplify with time as the timeline stretches. Timelines can be generated experimentally in a water channel through use of a **hydrogen bubble wire.** When a short burst of electric current is sent through the cathode wire, electrolysis of the water occurs and tiny hydrogen gas bubbles form at the wire. Since the bubbles are so small, their buoyancy is nearly negligible, and the bubbles follow the water flow nicely (Fig. 4–28).

Refractive Flow Visualization Techniques

Another category of flow visualization is based on the **refractive property** of light waves. As you recall from your study of physics, the speed of light through one material may differ somewhat from that in another material, or even in the _same_ material if its density changes. As light travels through one fluid into a fluid with a different index of refraction, the light rays bend (they are **refracted**).

There are two primary flow visualization techniques that utilize the fact that the index of refraction in air (or other gases) varies with density. They are the **shadowgraph technique** and the **schlieren technique** (Settles, 2001). **Interferometry** is a visualization technique that utilizes the related _phase change_ of light as it passes through air of varying densities as the basis for flow visualization and is not discussed here (see Merzkirch, 1987). All these techniques are useful for flow visualization in flow fields where density changes from one location in the flow to another, such as natural convection flows (temperature differences cause the density variations), mixing flows (fluid species cause the density variations), and supersonic flows (shock waves and expansion waves cause the density variations).

Unlike flow visualizations involving streaklines, pathlines, and timelines, the shadowgraph and schlieren methods do not require injection of a visible
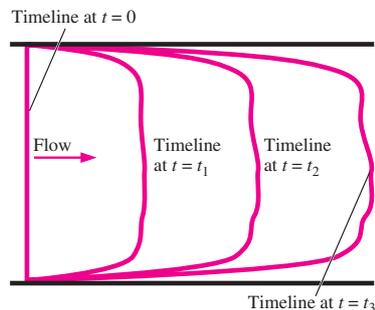
FIGURE 4–27
Timelines are formed by marking a line of fluid particles, and then watching that line move (and deform) through the flow field; timelines are shown at $t = 0$, t_1, t_2, and t_3.
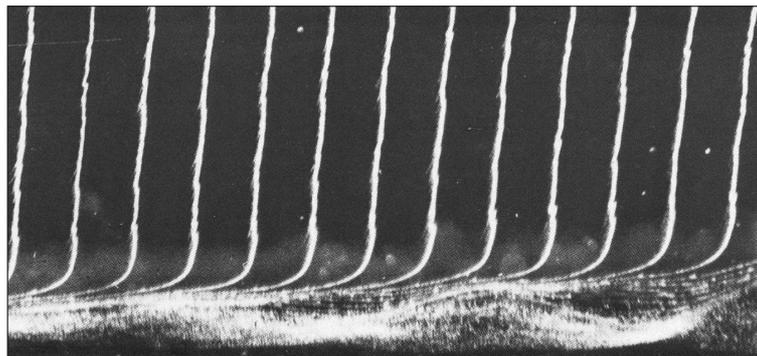
FIGURE 4–28
Timelines produced by a hydrogen bubble wire are used to visualize the boundary layer velocity profile shape. Flow is from left to right, and the hydrogen bubble wire is located to the left of the field of view. Bubbles near the wall reveal a flow instability that leads to turbulence.

Bippes, H. 1972 Sitzungsber, Heidelb. Akad. Wiss. Math. Naturwiss. _Kl., no. 3, 103–180; NASA TM-75243, 1978._
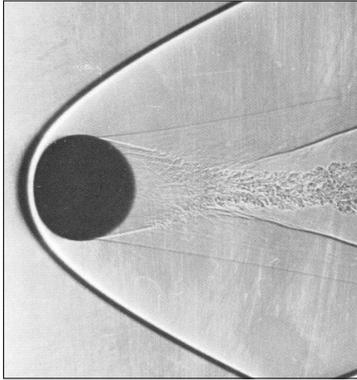
FIGURE 4–29
Shadowgram of a 14.3 mm sphere in free flight through air at Ma = 3.0. A shock wave is clearly visible in the shadow as a dark band that curves around the sphere and is called a *bow wave* (see Chap. 12).

A. C. Charters, Air Flow Branch, U.S. Army Ballistic Research Laboratory.

FIGURE 4–30
Schlieren image of natural convection due to a barbeque grill.

G. S. Settles, Gas Dynamics Lab, Penn State University. Used by permission.

tracer (smoke or dye). Rather, density differences and the refractive property of light provide the necessary means for visualizing regions of activity in the flow field, allowing us to "see the invisible." The image (a **shadowgram**) produced by the shadowgraph method is formed when the refracted rays of light rearrange the shadow cast onto a viewing screen or camera focal plane, causing bright or dark patterns to appear in the shadow. The dark patterns indicate the location where the refracted rays *originate*, while the bright patterns mark where these rays *end up*, and can be misleading. As a result, the dark regions are less distorted than the bright regions and are more useful in the interpretation of the shadowgram. In the shadowgram of Fig. 4–29, for example, we can be confident of the shape and position of the bow shock wave (the dark band), but the refracted bright light has distorted the front of the sphere's shadow.

A shadowgram is not a true optical image; it is, after all, merely a shadow. A **schlieren image,** however, involves lenses (or mirrors) and a knife edge or other cutoff device to block the refracted light and is a true focused optical image. Schlieren imaging is more complicated to set up than is shadowgraphy (see Settles, 2001, for details) but has a number of advantages. For example, a schlieren image does not suffer from optical distortion by the refracted light rays. Schlieren imaging is also more sensitive to weak density gradients such as those caused by natural convection (Fig. 4–30) or by gradual phenomena like expansion fans in supersonic flow. Color schlieren imaging techniques have also been developed. Finally, one can adjust more components in a schlieren setup, such as the location, orientation, and type of the cutoff device, in order to produce an image that is most useful for the problem at hand.

Surface Flow Visualization Techniques

Finally, we briefly mention some flow visualization techniques that are useful along solid surfaces. The direction of fluid flow immediately above a solid surface can be visualized with **tufts**—short, flexible strings glued to the surface at one end that point in the flow direction. Tufts are especially useful for locating regions of flow separation, where the flow direction suddenly reverses.

A technique called **surface oil visualization** can be used for the same purpose—oil placed on the surface forms streaks that indicate the direction of flow. If it rains lightly when your car is dirty (especially in the winter when salt is on the roads), you may have noticed streaks along the hood and sides of the car, or even on the windshield. This is similar to what is observed with surface oil visualization.

Lastly, there are pressure-sensitive and temperature-sensitive paints that enable researchers to observe the pressure or temperature distribution along solid surfaces.

4–3 ▪ PLOTS OF FLUID FLOW DATA

Regardless of how the results are obtained (analytically, experimentally, or computationally), it is usually necessary to *plot* flow data in ways that enable the reader to get a feel for how the flow properties vary in time and/or space. You are already familiar with *time plots*, which are especially

useful in turbulent flows (e.g., a velocity component plotted as a function of time), and *xy*-plots (e.g., pressure as a function of radius). In this section, we discuss three additional types of plots that are useful in fluid mechanics—profile plots, vector plots, and contour plots.

Profile Plots

> A **profile plot** indicates how the value of a scalar property varies along some desired direction in the flow field.

Profile plots are the simplest of the three to understand because they are like the common *xy*-plots that you have generated since grade school. Namely, you plot how one variable *y* varies as a function of a second variable *x*. In fluid mechanics, profile plots of *any* scalar variable (pressure, temperature, density, etc.) can be created, but the most common one used in this book is the *velocity profile plot*. We note that since velocity is a vector quantity, we usually plot either the magnitude of velocity or one of the components of the velocity vector as a function of distance in some desired direction.

For example, one of the timelines in the boundary layer flow of Fig. 4–28 can be converted into a velocity profile plot by recognizing that at a given instant in time, the horizontal distance traveled by a hydrogen bubble at vertical location *y* is proportional to the local *x*-component of velocity *u*. We plot *u* as a function of *y* in Fig. 4–31. The values of *u* for the plot can also be obtained analytically (see Chaps. 9 and 10), experimentally using PIV or some kind of local velocity measurement device (see Chap. 8), or computationally (see Chap. 15). Note that it is more physically meaningful in this example to plot *u* on the *abscissa* (horizontal axis) rather than on the *ordinate* (vertical axis) even though it is the dependent variable, since position *y* is then in its proper orientation (up) rather than across.

Finally, it is common to add arrows to velocity profile plots to make them more visually appealing, although no additional information is provided by the arrows. If more than one component of velocity is plotted by the arrow, the *direction* of the local velocity vector is indicated and the velocity profile plot becomes a velocity *vector* plot.

Vector Plots

> A **vector plot** is an array of arrows indicating the magnitude and direction of a vector property at an instant in time.

While streamlines indicate the *direction* of the instantaneous velocity field, they do not directly indicate the *magnitude* of the velocity (i.e., the speed). A useful flow pattern for both experimental and computational fluid flows is thus the vector plot, which consists of an array of arrows that indicate both magnitude *and* direction of an instantaneous vector property. We have already seen an example of a velocity vector plot in Fig. 4–4 and an acceleration vector plot in Fig. 4–14. These were generated analytically. Vector plots can also be generated from experimentally obtained data (e.g., from PIV measurements) or numerically from CFD calculations.

To further illustrate vector plots, we generate a two-dimensional flow field consisting of free-stream flow impinging on a block of rectangular cross section. We perform CFD calculations, and the results are shown in
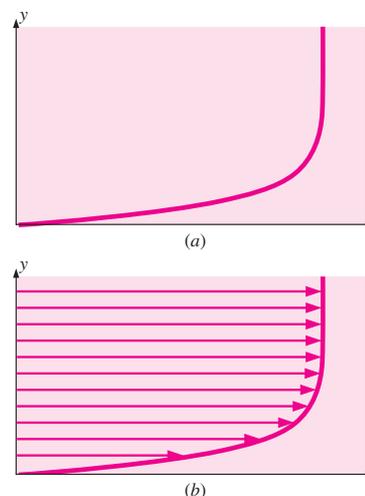
FIGURE 4–31
Profile plots of the horizontal component of velocity as a function of vertical distance; flow in the boundary layer growing along a horizontal flat plate: (*a*) standard profile plot and (*b*) profile plot with arrows.

FLOW

Recirculating eddy

Block

Symmetry plane

(*a*)

FLOW

Block

(*b*)
Symmetry plane

Block

(*c*)
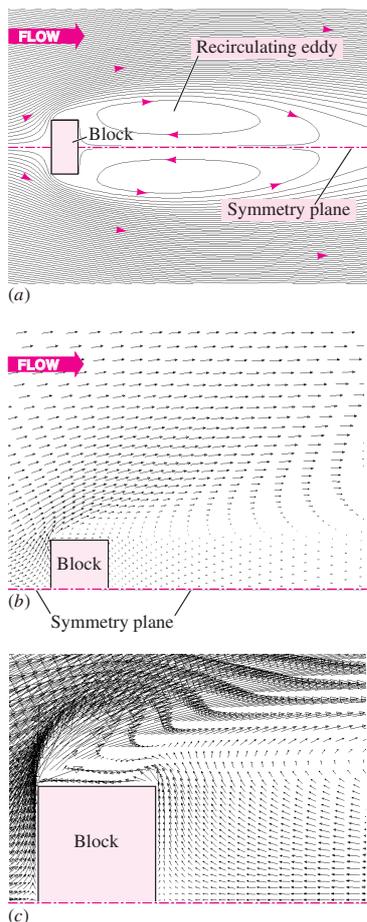
FIGURE 4–32
Results of CFD calculations of flow impinging on a block; (*a*) streamlines, (*b*) velocity vector plot of the upper half of the flow, and (*c*) velocity vector plot, close-up view revealing more details.

Fig. 4–32. Note that this flow is by nature turbulent and unsteady, but only the long-time averaged results are calculated and displayed here. Streamlines are plotted in Fig. 4–32*a*; a view of the entire block and a large portion of its wake is shown. The closed streamlines above and below the symmetry plane indicate large recirculating eddies, one above and one below the line of symmetry. A velocity vector plot is shown in Fig. 4–32*b*. (Only the upper half of the flow is shown because of symmetry.) It is clear from this plot that the flow accelerates around the upstream corner of the block, so much so in fact that the boundary layer cannot negotiate the sharp corner and separates off the block, producing the large recirculating eddies downstream of the block. (Note that these velocity vectors are time-averaged values; the instantaneous vectors change in both magnitude and direction with time as vortices are shed from the body, similar to those of Fig. 4–25*a*.) A close-up view of the separated flow region is plotted in Fig. 4–32*c*, where we verify the reverse flow in the lower half of the large recirculating eddy.

Modern CFD codes and postprocessors can add *color* to a vector plot. For example, the vectors can be colored according to some other flow property such as pressure (red for high pressure and blue for low pressure) or temperature (red for hot and blue for cold). In this manner, one can easily visualize not only the magnitude and direction of the flow, but other properties as well, simultaneously.

Contour Plots

> A **contour plot** shows curves of constant values of a scalar property (or magnitude of a vector property) at an instant in time.

If you do any hiking, you are familiar with contour maps of mountain trails. The maps consist of a series of closed curves, each indicating a constant elevation or altitude. Near the center of a group of such curves is the mountain peak or valley; the actual peak or valley is a *point* on the map showing the highest or lowest elevation. Such maps are useful in that not only do you get a bird's-eye view of the streams and trails, etc., but you can also easily see your elevation and where the trail is flat or steep. In fluid mechanics, the same principle is applied to various scalar flow properties; contour plots (also called **isocontour plots**) are generated of pressure, temperature, velocity magnitude, species concentration, properties of turbulence, etc. A contour plot can quickly reveal regions of high (or low) values of the flow property being studied.

A contour plot may consist simply of curves indicating various levels of the property; this is called a **contour line plot.** Alternatively, the contours can be filled in with either colors or shades of gray; this is called a **filled contour plot.** An example of pressure contours is shown in Fig. 4–33 for the same flow as in Fig. 4–32. In Fig. 4–33*a*, filled contours are shown using shades of gray to identify regions of different pressure levels—dark regions indicate low pressure and light regions indicate high pressure. It is clear from this figure that the pressure is highest at the front face of the block and lowest along the top of the block in the separated zone. The pressure is also low in the wake of the block, as expected. In Fig. 4–33*b*, the same pressure contours are shown, but as a contour line plot with labeled levels of gage pressure in units of pascals.

In CFD, contour plots are often displayed in vivid colors with red usually indicating the highest value of the scalar and blue the lowest. A healthy human eye can easily spot a red or blue region and thus locate regions of high or low value of the flow property. Because of the pretty pictures produced by CFD, computational fluid dynamics is sometimes given the nickname "colorful fluid dynamics."

4–4 ▪ OTHER KINEMATIC DESCRIPTIONS

Types of Motion or Deformation of Fluid Elements

In fluid mechanics, as in solid mechanics, an element may undergo four fundamental types of motion or deformation, as illustrated in two dimensions in Fig. 4–34: (*a*) **translation,** (*b*) **rotation,** (*c*) **linear strain** (sometimes called **extensional strain**), and (*d*) **shear strain.** The study of fluid dynamics is further complicated by the fact that all four types of motion or deformation usually occur simultaneously. Because fluid elements may be in constant motion, it is preferable in fluid dynamics to describe the motion and deformation of fluid elements in terms of *rates*. In particular, we discuss *velocity* (rate of translation), *angular velocity* (rate of rotation), *linear strain rate* (rate of linear strain), and *shear strain rate* (rate of shear strain). In order for these **deformation rates** to be useful in the calculation of fluid flows, we must express them in terms of velocity and derivatives of velocity.

Translation and rotation are easily understood since they are commonly observed in the motion of solid particles such as billiard balls (Fig. 4–1). A vector is required in order to fully describe the rate of translation in three dimensions. The **rate of translation vector** is described mathematically as the **velocity vector.** In Cartesian coordinates,

Rate of translation vector in Cartesian coordinates:

$$\vec{V} = u\vec{i} + v\vec{j} + w\vec{k} \qquad (4\text{–}19)$$

In Fig. 4–34*a*, the fluid element has moved in the positive horizontal (*x*) direction; thus *u* is positive, while *v* (and *w*) are zero.

Rate of rotation (**angular velocity**) at a point is defined as *the average rotation rate of two initially perpendicular lines that intersect at that point*. In Fig. 4–34*b*, for example, consider the point at the bottom-left corner of the initially square fluid element. The left edge and the bottom edge of the element intersect at that point and are initially perpendicular. Both of these lines rotate counterclockwise, which is the mathematically positive direction. The angle between these two lines (or between *any* two initially perpendicular lines on this fluid element) remains at 90° since solid body rotation is illustrated in the figure. Therefore, both lines rotate at the same rate, and the rate of rotation in the plane is simply the component of angular velocity in that plane.

In the more general, but still two-dimensional case (Fig. 4–35), the fluid particle translates and deforms as it rotates, and the rate of rotation is calculated according to the definition given in the previous paragraph. Namely, we begin at time t_1 with two initially perpendicular lines (lines *a* and *b* in Fig. 4–35) that intersect at point *P* in the *xy*-plane. We follow these lines as they move and rotate in an infinitesimal increment of time $dt = t_2 - t_1$. At
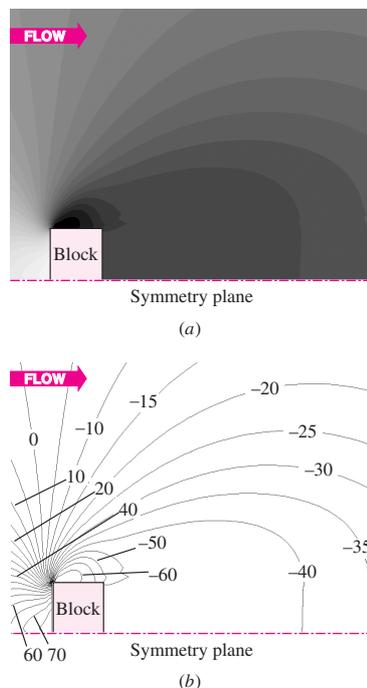
FIGURE 4–33

Contour plots of the pressure field due to flow impinging on a block, as produced by CFD calculations; only the upper half is shown due to symmetry; (*a*) filled gray scale contour plot and (*b*) contour line plot where pressure values are displayed in units of Pa (pascals) gage pressure.
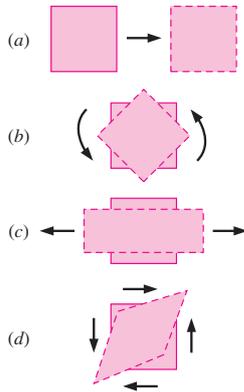
FIGURE 4–34
Fundamental types of fluid element
motion or deformation: (*a*) translation,
(*b*) rotation, (*c*) linear strain, and
(*d*) shear strain.

time t_2, line *a* has rotated by angle α_a, and line *b* has rotated by angle α_b, and both lines have moved with the flow as sketched (both angle values are given in radians and are shown mathematically positive in the sketch). The average rotation angle is thus $(\alpha_a + \alpha_b)/2$, and the *rate of rotation* or angular velocity in the *xy*-plane is equal to the time derivative of this average rotation angle,

Rate of rotation of fluid element about point P in Fig. 4–35:

$$\omega = \frac{d}{dt}\left(\frac{\alpha_a + \alpha_b}{2}\right) = \frac{1}{2}\left(\frac{\partial v}{\partial x} - \frac{\partial u}{\partial y}\right) \tag{4–20}$$

It is left as an exercise to prove the right side of Eq. 4–20 where we have written ω in terms of velocity components *u* and *v* in place of angles α_a and α_b.

In three dimensions, we must define a *vector* for the rate of rotation at a point in the flow since its magnitude may differ in each of the three dimensions. Derivation of the rate of rotation vector in three dimensions can be found in many fluid mechanics books such as Kundu (1990) and White (1991). The **rate of rotation vector** is equal to the **angular velocity vector** and is expressed in Cartesian coordinates as

Rate of rotation vector in Cartesian coordinates:

$$\vec{\omega} = \frac{1}{2}\left(\frac{\partial w}{\partial y} - \frac{\partial v}{\partial z}\right)\vec{i} + \frac{1}{2}\left(\frac{\partial u}{\partial z} - \frac{\partial w}{\partial x}\right)\vec{j} + \frac{1}{2}\left(\frac{\partial v}{\partial x} - \frac{\partial u}{\partial y}\right)\vec{k} \tag{4–21}$$

Linear strain rate is defined as *the rate of increase in length per unit length*. Mathematically, the linear strain rate of a fluid element depends on the initial orientation or direction of the line segment upon which we measure the linear strain. Thus, it cannot be expressed as a scalar or vector quantity. Instead, we define linear strain rate in some arbitrary direction, which we denote as the x_α-direction. For example, line segment *PQ* in Fig. 4–36 has an initial length of dx_α, and it grows to line segment $P'Q'$ as shown. From the given definition and using the lengths marked in Fig. 4–36, the linear strain rate in the x_α-direction is

$$\varepsilon_{\alpha\alpha} = \frac{d}{dt}\left(\frac{P'Q' - PQ}{PQ}\right)$$

$$\cong \frac{d}{dt}\left(\frac{\overbrace{\left(u_\alpha + \frac{\partial u_\alpha}{\partial x_\alpha}dx_\alpha\right)dt + dx_\alpha - u_\alpha\,dt}^{\text{Length of } P'Q' \text{ in the } x_\alpha\text{-direction}} - \overbrace{dx_\alpha}^{\text{Length of } PQ \text{ in the } x_\alpha\text{-direction}}}{\underbrace{dx_\alpha}_{\text{Length of } PQ \text{ in the } x_\alpha\text{-direction}}}\right) = \frac{\partial u_\alpha}{\partial x_\alpha} \tag{4–22}$$

In Cartesian coordinates, we normally take the x_α-direction as that of each of the three coordinate axes, although we are not restricted to these directions.

Linear strain rate in Cartesian coordinates:

$$\varepsilon_{xx} = \frac{\partial u}{\partial x} \qquad \varepsilon_{yy} = \frac{\partial v}{\partial y} \qquad \varepsilon_{zz} = \frac{\partial w}{\partial z} \tag{4–23}$$

For the more general case, the fluid element moves and deforms as sketched in Fig. 4–35. It is left as an exercise to show that Eq. 4–23 is still valid for the general case.
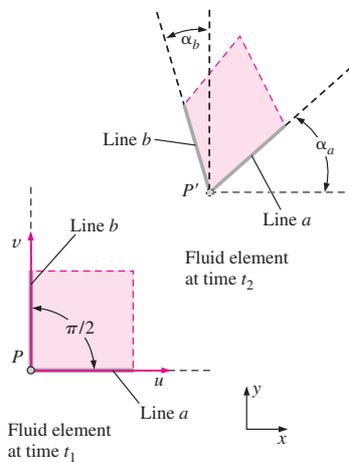
FIGURE 4–35
For a fluid element that translates
and deforms as sketched, the *rate of
rotation* at point *P* is defined as the
average rotation rate of two initially
perpendicular lines (lines *a* and *b*).

Solid objects such as wires, rods, and beams stretch when pulled. You should recall from your study of engineering mechanics that when such an object stretches in one direction, it usually shrinks in direction(s) normal to that direction. The same is true of fluid elements. In Fig. 4–34*c*, the originally square fluid element stretches in the horizontal direction and shrinks in the vertical direction. The linear strain rate is thus positive horizontally and negative vertically.

If the flow is *incompressible*, the net volume of the fluid element must remain constant; thus if the element stretches in one direction, it must shrink by an appropriate amount in other direction(s) to compensate. The volume of a *compressible* fluid element, however, may increase or decrease as its density decreases or increases, respectively. (The mass of a fluid element must remain constant, but since $\rho = m/V$, density and volume are inversely proportional.) Consider for example a parcel of air in a cylinder being compressed by a piston (Fig. 4–37); the volume of the fluid element decreases while its density increases such that the fluid element's mass is conserved. The rate of increase of volume of a fluid element per unit volume is called its **volumetric strain rate** or **bulk strain rate.** This kinematic property is defined as *positive* when the volume *increases*. Another synonym of volumetric strain rate is **rate of volumetric dilatation,** which is easy to remember if you think about how the iris of your eye dilates (enlarges) when exposed to dim light. It turns out that the volumetric strain rate is the sum of the linear strain rates in three mutually orthogonal directions. In Cartesian coordinates (Eq. 4–23), the volumetric strain rate is thus

Volumetric strain rate in Cartesian coordinates:

$$\frac{1}{V}\frac{DV}{Dt} = \frac{1}{V}\frac{dV}{dt} = \varepsilon_{xx} + \varepsilon_{yy} + \varepsilon_{zz} = \frac{\partial u}{\partial x} + \frac{\partial v}{\partial y} + \frac{\partial w}{\partial z} \qquad \textbf{(4–24)}$$

In Eq. 4–24, the uppercase *D* notation is used to stress that we are talking about the volume *following a fluid element*, that is to say, the *material volume* of the fluid element, as in Eq. 4–12.

The volumetric strain rate is zero in an incompressible flow.

Shear strain rate is a more difficult deformation rate to describe and understand. **Shear strain rate** at a point is defined as *half of the rate of decrease of the angle between two initially perpendicular lines that intersect at the point*. (The reason for the half will become clear later when we combine shear strain rate and linear strain rate into one tensor.) In Fig. 4–34*d*, for example, the initially 90° angles at the lower-left corner and upper-right corner of the square fluid element decrease; this is by definition a *positive* shear strain. However, the angles at the upper-left and lower-right corners of the square fluid element increase as the initially square fluid element deforms; this is a *negative* shear strain. Obviously we cannot describe the shear strain rate in terms of only one scalar quantity or even in terms of one *vector* quantity for that matter. Rather, a full mathematical description of shear strain rate requires its specification in any *two mutually perpendicular directions*. In Cartesian coordinates, the axes themselves are the most obvious choice, although we are not restricted to these. Consider a fluid element in two dimensions in the *xy*-plane. The element translates and deforms with time as sketched in Fig. 4–38. Two initially mutually perpendicular
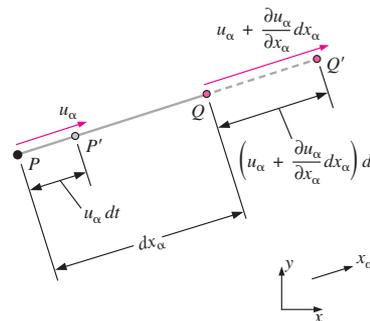
FIGURE 4–36
Linear strain rate in some arbitrary direction x_α is defined as the rate of increase in length per unit length in that direction. Linear strain rate would be *negative* if the line segment length were to *decrease*. Here we follow the increase in length of line segment PQ into line segment $P'Q'$, which yields a positive linear strain rate. Velocity components and distances are truncated to first-order since dx_α and dt are infinitesimally small.

Time t_1 Time t_2
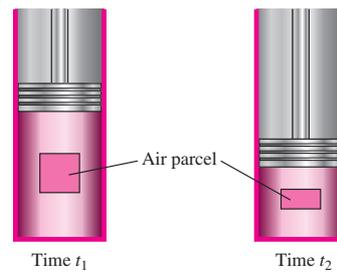
FIGURE 4–37
Air being compressed by a piston in a cylinder; the volume of a fluid element in the cylinder decreases, corresponding to a negative rate of volumetric dilatation.
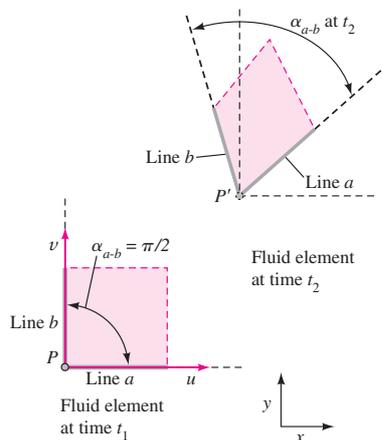
FIGURE 4–38
For a fluid element that translates and deforms as sketched, the *shear strain rate* at point P is defined as half of the rate of decrease of the angle between two initially perpendicular lines (lines a and b).
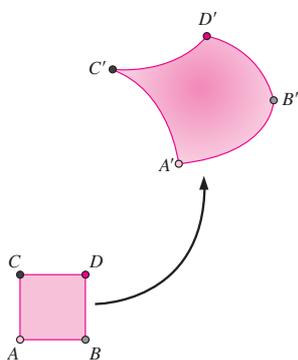
FIGURE 4–39
A fluid element illustrating translation, rotation, linear strain, shear strain, and volumetric strain.

lines (lines a and b in the x- and y-directions, respectively) are followed. The angle between these two lines decreases from $\pi/2$ (90°) to the angle marked $\alpha_{a\text{-}b}$ at t_2 in the sketch. It is left as an exercise to show that the shear strain rate at point P for initially perpendicular lines in the x- and y-directions is given by

Shear strain rate, initially perpendicular lines in the x- and y-directions:

$$\varepsilon_{xy} = -\frac{1}{2}\frac{d}{dt}\alpha_{a\text{-}b} = \frac{1}{2}\left(\frac{\partial u}{\partial y} + \frac{\partial v}{\partial x}\right) \tag{4–25}$$

Equation 4–25 can be easily extended to three dimensions. The shear strain rate is thus

Shear strain rate in Cartesian coordinates:

$$\varepsilon_{xy} = \frac{1}{2}\left(\frac{\partial u}{\partial y} + \frac{\partial v}{\partial x}\right) \qquad \varepsilon_{zx} = \frac{1}{2}\left(\frac{\partial w}{\partial x} + \frac{\partial u}{\partial z}\right) \qquad \varepsilon_{yz} = \frac{1}{2}\left(\frac{\partial v}{\partial z} + \frac{\partial w}{\partial y}\right) \tag{4–26}$$

Finally, it turns out that we can mathematically combine linear strain rate and shear strain rate into one symmetric second-order tensor called the **strain rate tensor,** which is a combination of Eqs. 4–23 and 4–26:

Strain rate tensor in Cartesian coordinates:

$$\varepsilon_{ij} = \begin{pmatrix} \varepsilon_{xx} & \varepsilon_{xy} & \varepsilon_{xz} \\ \varepsilon_{yx} & \varepsilon_{yy} & \varepsilon_{yz} \\ \varepsilon_{zx} & \varepsilon_{zy} & \varepsilon_{zz} \end{pmatrix} = \begin{pmatrix} \dfrac{\partial u}{\partial x} & \dfrac{1}{2}\left(\dfrac{\partial u}{\partial y} + \dfrac{\partial v}{\partial x}\right) & \dfrac{1}{2}\left(\dfrac{\partial u}{\partial z} + \dfrac{\partial w}{\partial x}\right) \\ \dfrac{1}{2}\left(\dfrac{\partial v}{\partial x} + \dfrac{\partial u}{\partial y}\right) & \dfrac{\partial v}{\partial y} & \dfrac{1}{2}\left(\dfrac{\partial v}{\partial z} + \dfrac{\partial w}{\partial y}\right) \\ \dfrac{1}{2}\left(\dfrac{\partial w}{\partial x} + \dfrac{\partial u}{\partial z}\right) & \dfrac{1}{2}\left(\dfrac{\partial w}{\partial y} + \dfrac{\partial v}{\partial z}\right) & \dfrac{\partial w}{\partial z} \end{pmatrix} \tag{4–27}$$

The strain rate tensor obeys all the laws of mathematical tensors, such as tensor invariants, transformation laws, and principal axes.

Figure 4–39 shows a general (although two-dimensional) situation in a compressible fluid flow in which all possible motions and deformations are present simultaneously. In particular, there is translation, rotation, linear strain, and shear strain. Because of the compressible nature of the fluid, there is also volumetric strain (dilatation). You should now have a better appreciation of the inherent complexity of fluid dynamics, and the mathematical sophistication required to fully describe fluid motion.

EXAMPLE 4–6   Calculation of Kinematic Properties in a Two-Dimensional Flow

Consider the steady, two-dimensional velocity field of Example 4–1:

$$\vec{V} = (u, v) = (0.5 + 0.8\,x)\vec{i} + (1.5 - 0.8\,y)\vec{j} \tag{1}$$

where lengths are in units of m, time in s, and velocities in m/s. There is a stagnation point at $(-0.625, 1.875)$ as shown in Fig. 4–40. Streamlines of the flow are also plotted in Fig. 4–40. Calculate the various kinematic properties, namely, the rate of translation, rate of rotation, linear strain rate, shear strain rate, and volumetric strain rate. Verify that this flow is incompressible.

SOLUTION We are to calculate several kinematic properties of a given velocity field and verify that the flow is incompressible.

Assumptions **1** The flow is steady. **2** The flow is two-dimensional, implying no z-component of velocity and no variation of u or v with z.

Analysis By Eq. 4–19, the rate of translation is simply the velocity vector itself, given by Eq. 1. Thus,

Rate of translation: $u = 0.5 + 0.8x$ $v = 1.5 − 0.8y$ $w = 0$ **(2)**

The rate of rotation is found from Eq. 4–21. In this case, since $w = 0$ everywhere, and since neither u nor v vary with z, the only nonzero component of rotation rate is in the z-direction. Thus,

Rate of rotation: $\vec{\omega} = \dfrac{1}{2}\left(\dfrac{\partial v}{\partial x} - \dfrac{\partial u}{\partial y}\right)\vec{k} = \dfrac{1}{2}(0 - 0)\vec{k} = \mathbf{0}$ **(3)**

In this case, we see that there is no net rotation of fluid particles as they move about. (This is a significant piece of information, to be discussed in more detail later in this chapter and also in Chap. 10.)

Linear strain rates can be calculated in any arbitrary direction using Eq. 4–22. In the x-, y-, and z-directions, the linear strain rates of Eq. 4–23 are

$$\varepsilon_{xx} = \frac{\partial u}{\partial x} = \mathbf{0.8\ s^{-1}} \qquad \varepsilon_{yy} = \frac{\partial v}{\partial y} = \mathbf{-0.8\ s^{-1}} \qquad \varepsilon_{zz} = \mathbf{0} \qquad \textbf{(4)}$$

Thus, we predict that fluid particles *stretch* in the x-direction (positive linear strain rate) and *shrink* in the y-direction (negative linear strain rate). This is illustrated in Fig. 4–41, where we have marked an initially square parcel of fluid centered at (0.25, 4.25). By integrating Eqs. 2 with time, we calculate the location of the four corners of the marked fluid after an elapsed time of 1.5 s. Indeed this fluid parcel has stretched in the x-direction and has shrunk in the y-direction as predicted.

Shear strain rate is determined from Eq. 4–26. Because of the two-dimensionality, nonzero shear strain rates can occur only in the xy-plane. Using lines parallel to the x- and y-axes as our initially perpendicular lines, we calculate ε_{xy} from Eq. 4–26:

$$\varepsilon_{xy} = \frac{1}{2}\left(\frac{\partial u}{\partial y} + \frac{\partial v}{\partial x}\right) = \frac{1}{2}(0 + 0) = \mathbf{0} \qquad \textbf{(5)}$$

Thus, there is no shear strain in this flow, as also indicated by Fig. 4–41. Although the sample fluid particle deforms, it remains rectangular; its initially 90° corner angles remain at 90° throughout the time period of the calculation.

Finally, the volumetric strain rate is calculated from Eq. 4–24:

$$\frac{1}{V}\frac{DV}{Dt} = \varepsilon_{xx} + \varepsilon_{yy} + \varepsilon_{zz} = (0.8 - 0.8 + 0)\ \text{s}^{-1} = \mathbf{0} \qquad \textbf{(6)}$$

Since the volumetric strain rate is zero everywhere, we can say definitively that fluid particles are neither dilating (expanding) nor shrinking (compressing) in volume. Thus, **we verify that this flow is indeed incompressible**. In Fig. 4–41, the area of the shaded fluid particle remains constant as it moves and deforms in the flow field.

Discussion In this example it turns out that the linear strain rates (ε_{xx} and ε_{yy}) are nonzero, while the shear strain rates (ε_{xy} and its symmetric partner ε_{yx})
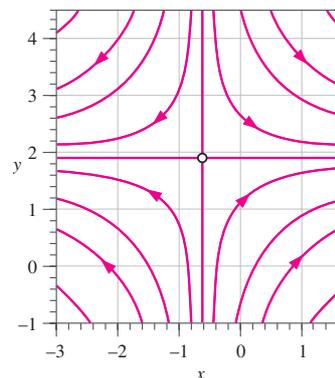
FIGURE 4–40
Streamlines for the velocity field of Example 4–6. The stagnation point is indicated by the circle at $x = -0.625$ m and $y = 1.875$ m.
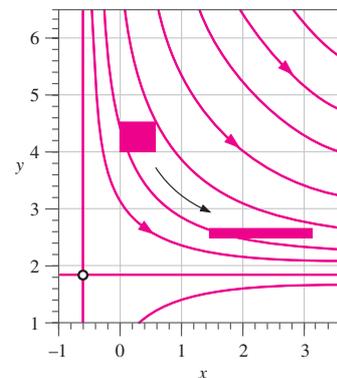
FIGURE 4–41
Deformation of an initially square parcel of marked fluid subjected to the velocity field of Example 4–6 for a time period of 1.5 s. The stagnation point is indicated by the circle at $x = -0.625$ m and $y = 1.875$ m, and several streamlines are plotted.

$$\vec{C} = \vec{A} \times \vec{B}$$
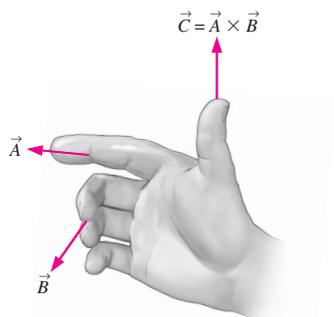
FIGURE 4–42
The direction of a vector cross product is determined by the right-hand rule.

are zero. This means that *the x- and y-axes of this flow field are the principal axes.* The (two-dimensional) strain rate tensor in this orientation is thus

$$\varepsilon_{ij} = \begin{pmatrix} \varepsilon_{xx} & \varepsilon_{xy} \\ \varepsilon_{yx} & \varepsilon_{yy} \end{pmatrix} = \begin{pmatrix} 0.8 & 0 \\ 0 & -0.8 \end{pmatrix} \text{s}^{-1} \tag{7}$$

If we were to rotate the axes by some arbitrary angle, the new axes would *not* be principal axes, and all four elements of the strain rate tensor would be nonzero. You may recall rotating axes in your engineering mechanics classes through use of Mohr's circles to determine principal axes, maximum shear strains, etc. Similar analyses can be performed in fluid mechanics.

Vorticity and Rotationality

We have already defined the rate of rotation vector of a fluid element (see Eq. 4–21). A closely related kinematic property is of great importance to the analysis of fluid flows. Namely, the **vorticity vector** is defined mathematically as the curl of the velocity vector $\vec{V}$,

Vorticity vector:
$$\vec{\zeta} = \vec{\nabla} \times \vec{V} = \text{curl}(\vec{V}) \tag{4–28}$$

Physically, you can tell the direction of the vorticity vector by using the right-hand rule for cross product (Fig. 4–42). The symbol ζ used for vorticity is the Greek letter *zeta*. You should note that this symbol for vorticity is *not* universal among fluid mechanics textbooks; some authors use the Greek letter *omega* (ω) while still others use uppercase *omega* (Ω). In this book, $\vec{\omega}$ is used to denote the rate of rotation vector (angular velocity vector) of a fluid element. It turns out that the rate of rotation vector is equal to half of the vorticity vector,

Rate of rotation vector:
$$\vec{\omega} = \frac{1}{2} \vec{\nabla} \times \vec{V} = \frac{1}{2} \text{curl}(\vec{V}) = \frac{\vec{\zeta}}{2} \tag{4–29}$$

Thus, *vorticity is a measure of rotation of a fluid particle.* Specifically,

Vorticity is equal to twice the angular velocity of a fluid particle (Fig. 4–43).

If the vorticity at a point in a flow field is nonzero, the fluid particle that happens to occupy that point in space is rotating; the flow in that region is called **rotational.** Likewise, if the vorticity in a region of the flow is zero (or negligibly small), fluid particles there are not rotating; the flow in that region is called **irrotational.** Physically, fluid particles in a rotational region of flow rotate end over end as they move along in the flow. For example, fluid particles within the viscous boundary layer near a solid wall are rotational (and thus have nonzero vorticity), while fluid particles outside the boundary layer are irrotational (and their vorticity is zero). Both of these cases are illustrated in Fig. 4–44.

Rotation of fluid elements is associated with wakes, boundary layers, flow through turbomachinery (fans, turbines, compressors, etc.), and flow with heat transfer. The vorticity of a fluid element cannot change except through the action of viscosity, nonuniform heating (temperature gradients), or other nonuniform phenomena. Thus if a flow originates in an irrotational region, it remains irrotational until some nonuniform process alters it. For example,

FIGURE 4–43
The *vorticity vector* is equal to twice the angular velocity vector of a rotating fluid particle.
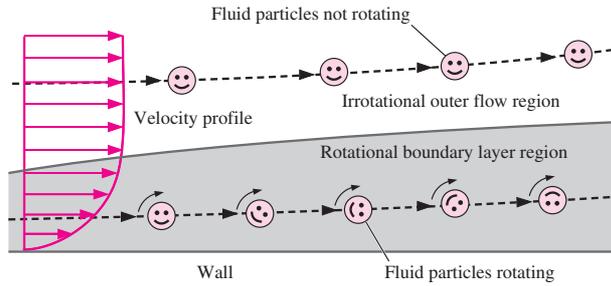
FIGURE 4–44
The difference between rotational and irrotational flow: fluid elements in a rotational region of the flow rotate, but those in an irrotational region of the flow do not.

FIGURE 4–45
For a two-dimensional flow in the *xy*-plane, the vorticity vector always points in the *z*- or −*z*-direction. In this illustration, the flag-shaped fluid particle rotates in the counterclockwise direction as it moves in the *xy*-plane; its vorticity points in the positive *z*-direction as shown.

air entering an inlet from quiescent (still) surroundings is irrotational and remains so unless it encounters an object in its path or is subjected to nonuniform heating. If a region of flow can be approximated as irrotational, the equations of motion are greatly simplified, as you will see in Chap. 10.

In Cartesian coordinates, $(\vec{i}, \vec{j}, \vec{k})$, (x, y, z), and (u, v, w), Eq. 4–28 can be expanded as follows:

Vorticity vector in Cartesian coordinates:

$$\vec{\zeta} = \left(\frac{\partial w}{\partial y} - \frac{\partial v}{\partial z}\right)\vec{i} + \left(\frac{\partial u}{\partial z} - \frac{\partial w}{\partial x}\right)\vec{j} + \left(\frac{\partial v}{\partial x} - \frac{\partial u}{\partial y}\right)\vec{k} \qquad \text{(4–30)}$$

If the flow is two-dimensional in the *xy*-plane, the *z*-component of velocity (w) is zero and neither u nor v varies with z. Thus the first two components of Eq. 4–30 are identically zero and the vorticity reduces to

Two-dimensional flow in Cartesian coordinates:

$$\vec{\zeta} = \left(\frac{\partial v}{\partial x} - \frac{\partial u}{\partial y}\right)\vec{k} \qquad \text{(4–31)}$$

Note that if a flow is two-dimensional in the *xy*-plane, the vorticity vector must point in either the *z*- or −*z*-direction (Fig. 4–45).

EXAMPLE 4–7   Vorticity Contours in a Two-Dimensional Flow

Consider the CFD calculation of two-dimensional free-stream flow impinging on a block of rectangular cross section, as shown in Figs. 4–32 and 4–33. Plot vorticity contours and discuss.

SOLUTION   We are to calculate the vorticity field for a given velocity field produced by CFD and then generate a contour plot of vorticity.
Analysis   Since the flow is two-dimensional, the only nonzero component of vorticity is in the *z*-direction, normal to the page in Figs. 4–32 and 4–33. A contour plot of the *z*-component of vorticity for this flow field is shown in Fig. 4–46. The dark region near the upper-left corner of the block indicates large negative values of vorticity, implying *clockwise* rotation of fluid particles in that region. This is due to the large velocity gradients encountered in this portion of the flow field; the boundary layer separates off the wall at the corner of

FIGURE 4–46
Contour plot of the vorticity field ζ_z due to flow impinging on a block, as produced by CFD calculations; only the upper half is shown due to symmetry. Dark regions represent large negative vorticity, and light regions represent large positive vorticity.
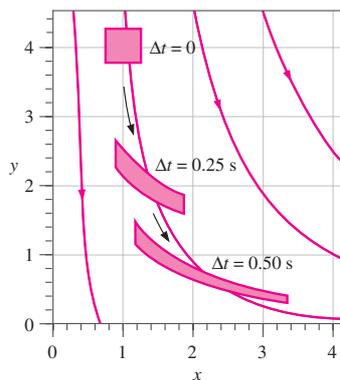
the body and forms a thin **shear layer** across which the velocity changes rapidly. The concentration of vorticity in the shear layer diminishes as vorticity diffuses downstream. The small lightly shaded region near the top right corner of the block represents a region of *positive* vorticity (counterclockwise rotation)—a secondary flow pattern caused by the flow separation.

Discussion We expect the magnitude of vorticity to be highest in regions where spatial derivatives of velocity are high (see Eq. 4–30). Close examination reveals that the dark region in Fig. 4–46 does indeed correspond to large velocity gradients in Fig. 4–32. Keep in mind that the vorticity field of Fig. 4–46 is time-averaged. The instantaneous flow field is in reality turbulent and unsteady, and vortices are shed from the bluff body.

EXAMPLE 4–8   **Determination of Rotationality
in a Two-Dimensional Flow**

Consider the following steady, incompressible, two-dimensional velocity field:

$$\vec{V} = (u, v) = x^2\vec{i} + (-2xy - 1)\vec{j} \tag{1}$$

Is this flow rotational or irrotational? Sketch some streamlines in the first quadrant and discuss.

SOLUTION We are to determine whether a flow with a given velocity field is rotational or irrotational, and we are to draw some streamlines in the first quadrant.

Analysis Since the flow is two-dimensional, Eq. 4–31 is valid. Thus,

Vorticity: $$\vec{\zeta} = \left(\frac{\partial v}{\partial x} - \frac{\partial u}{\partial y}\right)\vec{k} = (-2y - 0)\vec{k} = -2y\vec{k} \tag{2}$$

Since the vorticity is nonzero, this flow is **rotational.** In Fig. 4–47 we plot several streamlines of the flow in the first quadrant; we see that fluid moves downward and to the right. The translation and deformation of a fluid parcel is also shown: at $\Delta t = 0$, the fluid parcel is square, at $\Delta t = 0.25$ s, it has moved and deformed, and at $\Delta t = 0.50$ s, the parcel has moved farther and is further deformed. In particular, the right-most portion of the fluid parcel moves faster to the right and faster downward compared to the left-most portion, stretching the parcel in the x-direction and squashing it in the vertical direction. It is clear that there is also a net *clockwise* rotation of the fluid parcel, which agrees with the result of Eq. 2.

Discussion From Eq. 4–29, individual fluid particles rotate at an angular velocity equal to $\vec{\omega} = -y\vec{k}$, half of the vorticity vector. Since $\vec{\omega}$ is not constant, this flow is *not* solid-body rotation. Rather, $\vec{\omega}$ is a linear function of y. Further analysis reveals that this flow field is incompressible; the shaded areas representing the fluid parcel in Fig. 4–47 remain constant at all three instants in time.

FIGURE 4–47
Deformation of an initially square fluid parcel subjected to the velocity field of Example 4–8 for a time period of 0.25 s and 0.50 s. Several streamlines are also plotted in the first quadrant. It is clear that this flow is *rotational*.

In cylindrical coordinates, $(\vec{e}_r, \vec{e}_\theta, \vec{e}_z)$, (r, θ, z), and (u_r, u_θ, u_z), Eq. 4–28 can be expanded as

Vorticity vector in cylindrical coordinates:

$$\vec{\zeta} = \left(\frac{1}{r}\frac{\partial u_z}{\partial \theta} - \frac{\partial u_\theta}{\partial z}\right)\vec{e}_r + \left(\frac{\partial u_r}{\partial z} - \frac{\partial u_z}{\partial r}\right)\vec{e}_\theta + \frac{1}{r}\left(\frac{\partial(ru_\theta)}{\partial r} - \frac{\partial u_r}{\partial \theta}\right)\vec{e}_z \tag{4–32}$$

For two-dimensional flow in the $r\theta$-plane, Eq. 4–32 reduces to

Two-dimensional flow in cylindrical coordinates:

$$\vec{\zeta} = \frac{1}{r}\left(\frac{\partial(ru_\theta)}{\partial r} - \frac{\partial u_r}{\partial \theta}\right)\vec{k} \qquad \textbf{(4–33)}$$

where $\vec{k}$ is used as the unit vector in the z-direction in place of $\vec{e}_z$. Note that if a flow is two-dimensional in the $r\theta$-plane, the vorticity vector must point in either the z- or $-z$-direction (Fig. 4–48).

Comparison of Two Circular Flows

Not all flows with circular streamlines are rotational. To illustrate this point, we consider two incompressible, steady, two-dimensional flows, both of which have circular streamlines in the $r\theta$-plane:

Flow A—solid-body rotation: $\qquad u_r = 0 \qquad$ and $\qquad u_\theta = \omega r \qquad \textbf{(4–34)}$

Flow B—line vortex: $\qquad u_r = 0 \qquad$ and $\qquad u_\theta = \dfrac{K}{r} \qquad \textbf{(4–35)}$

where ω and K are constants. (Alert readers will note that u_θ in Eq. 4–35 is infinite at $r = 0$, which is of course physically impossible; we ignore the region close to the origin to avoid this problem.) Since the radial component of velocity is zero in both cases, the streamlines are circles about the origin. The velocity profiles for the two flows, along with their streamlines, are sketched in Fig. 4–49. We now calculate and compare the vorticity field for each of these flows, using Eq. 4–33.

Flow A—solid-body rotation: $\qquad \vec{\zeta} = \frac{1}{r}\left(\frac{\partial(\omega r^2)}{\partial r} - 0\right)\vec{k} = 2\omega\vec{k} \qquad \textbf{(4–36)}$

Flow B—line vortex: $\qquad \vec{\zeta} = \frac{1}{r}\left(\frac{\partial(K)}{\partial r} - 0\right)\vec{k} = 0 \qquad \textbf{(4–37)}$

Not surprisingly, the vorticity for solid-body rotation is nonzero. In fact, it is a constant of magnitude twice the angular velocity and pointing in the same direction. (This agrees with Eq. 4–29.) *Flow A is rotational*. Physically, this means that individual fluid particles rotate as they revolve around the origin (Fig. 4–49a). By contrast, the vorticity of the line vortex is identically zero everywhere (except right at the origin, which is a mathematical singularity). *Flow B is irrotational*. Physically, fluid particles do *not* rotate as they revolve in circles about the origin (Fig. 4–49b).

A simple analogy can be made between flow A and a merry-go-round or roundabout, and flow B and a Ferris wheel (Fig. 4–50). As children revolve around a roundabout, they also rotate at the same angular velocity as that of the ride itself. This is analogous to a rotational flow. In contrast, children on a Ferris wheel always remain oriented in an upright position as they trace out their circular path. This is analogous to an irrotational flow.
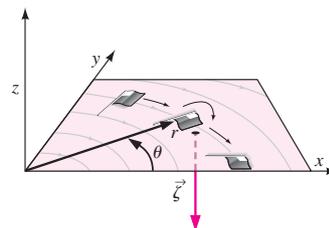
FIGURE 4–48
For a two-dimensional flow in the $r\theta$-plane, the vorticity vector always points in the z (or $-z$) direction. In this illustration, the flag-shaped fluid particle rotates in the clockwise direction as it moves in the $r\theta$-plane; its vorticity points in the $-z$-direction as shown.
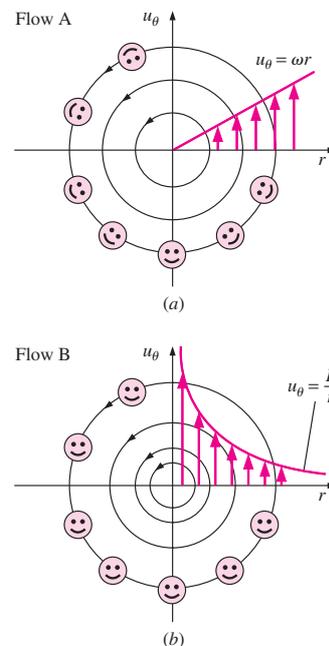
FIGURE 4–49
Streamlines and velocity profiles for (a) flow A, solid-body rotation and (b) flow B, a line vortex. Flow A is rotational, but flow B is irrotational everywhere except at the origin.

(a)   (b)

FIGURE 4–50
A simple analogy: (a) *rotational* circular flow is analogous to a roundabout,
while (b) *irrotational* circular flow is analogous to a Ferris wheel.
© Robb Gregg/PhotoEdit
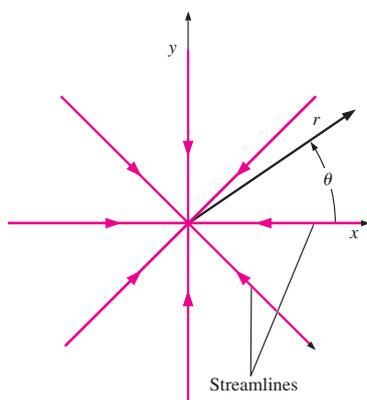
FIGURE 4–51
Streamlines in the $r\theta$-plane for the
case of a line sink.

EXAMPLE 4–9   Determination of Rotationality of a Line Sink

A simple two-dimensional velocity field called a **line sink** is often used to
simulate fluid being sucked into a line along the z-axis. Suppose the volume
flow rate per unit length along the z-axis, $\dot{V}/L$, is known, where $\dot{V}$ is a nega-
tive quantity. In two dimensions in the $r\theta$-plane,

Line sink: $u_r = \dfrac{\dot{V}}{2\pi L}\dfrac{1}{r}$ and $u_\theta = 0$ (1)

Draw several streamlines of the flow and calculate the vorticity. Is this flow
rotational or irrotational?

SOLUTION   Streamlines of the given flow field are to be sketched and the
rotationality of the flow is to be determined.
Analysis   Since there is only radial flow and no tangential flow, we know
immediately that all streamlines must be rays into the origin. Several stream-
lines are sketched in Fig. 4–51. The vorticity is calculated from Eq. 4–33:

$$\vec{\zeta} = \frac{1}{r}\left(\frac{\partial(ru_\theta)}{\partial r} - \frac{\partial}{\partial\theta}u_r\right)\vec{k} = \frac{1}{r}\left(0 - \frac{\partial}{\partial\theta}\left(\frac{\dot{V}}{2\pi L}\frac{1}{r}\right)\right)\vec{k} = 0 \qquad (2)$$

Since the vorticity vector is everywhere zero, this flow field is **irrotational**.
Discussion   Many practical flow fields involving suction, such as flow into
inlets and hoods, can be approximated quite accurately by assuming irrota-
tional flow (Heinsohn and Cimbala, 2003).

4–5 ▪ THE REYNOLDS TRANSPORT THEOREM

In thermodynamics and solid mechanics we often work with a **system** (also
called a **closed system**), defined as a *quantity of matter of fixed identity*. In
fluid dynamics, it is more common to work with a **control volume** (also

called an **open system**), defined as a *region in space chosen for study*. The size and shape of a system may change during a process, but no mass crosses its boundaries. A control volume, on the other hand, allows mass to flow in or out across its boundaries, which are called the **control surface.** A control volume may also move and deform during a process, but many real-world applications involve fixed, nondeformable control volumes.

Figure 4–52 illustrates both a system and a control volume for the case of deodorant being sprayed from a spray can. When analyzing the spraying process, a natural choice for our analysis is either the moving, deforming fluid (a system) or the volume bounded by the inner surfaces of the can (a control volume). These two choices are identical before the deodorant is sprayed. When some contents of the can are discharged, the system approach considers the discharged mass as part of the system and tracks it (a difficult job indeed); thus the mass of the system remains constant. Conceptually, this is equivalent to attaching a flat balloon to the nozzle of the can and letting the spray inflate the balloon. The inner surface of the balloon now becomes part of the boundary of the system. The control volume approach, however, is not concerned at all with the deodorant that has escaped the can (other than its properties at the exit), and thus the mass of the control volume decreases during this process while its volume remains constant. Therefore, the system approach treats the spraying process as an expansion of the system's volume, whereas the control volume approach considers it as a fluid discharge through the control surface of the fixed control volume.

Most principles of fluid mechanics are adopted from solid mechanics, where the physical laws dealing with the time rates of change of extensive properties are expressed for systems. In fluid mechanics, it is usually more convenient to work with control volumes, and thus there is a need to relate the changes in a control volume to the changes in a system. The relationship between the time rates of change of an extensive property for a system and for a control volume is expressed by the **Reynolds transport theorem (RTT)**, which provides the link between the system and control volume approaches (Fig. 4–53). RTT is named after the English engineer, Osborne Reynolds (1842–1912), who did much to advance its application in fluid mechanics.

The general form of the Reynolds transport theorem can be derived by considering a system with an arbitrary shape and arbitrary interactions, but the derivation is rather involved. To help you grasp the fundamental meaning of the theorem, we derive it first in a straightforward manner using a simple geometry and then generalize the results.

Consider flow from left to right through a diverging (expanding) portion of a flow field as sketched in Fig. 4–54. The upper and lower bounds of the fluid under consideration are *streamlines* of the flow, and we assume uniform flow through any cross section between these two streamlines. We choose the control volume to be fixed between sections (1) and (2) of the flow field. Both (1) and (2) are normal to the direction of flow. At some initial time t, the system coincides with the control volume, and thus the system and control volume are identical (the shaded region in Fig. 4–54). During time interval Δt, the system moves in the flow direction at uniform speeds V_1 at section (1) and V_2 at section (2). The system at this later time is indicated by the hatched region. The region uncovered by the system during
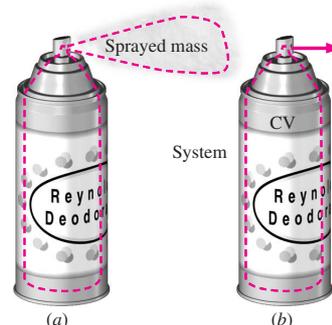
FIGURE 4–52
Two methods of analyzing the spraying of deodorant from a spray can: (*a*) We follow the fluid as it moves and deforms. This is the *system approach*—no mass crosses the boundary, and the total mass of the system remains fixed. (*b*) We consider a fixed interior volume of the can. This is the *control volume approach*—mass crosses the boundary.
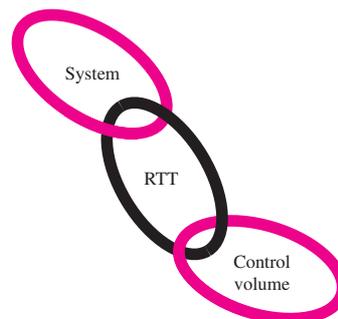
FIGURE 4–53
The *Reynolds transport theorem* (RTT) provides a link between the system approach and the control volume approach.

Control volume at time $t + \Delta t$
(CV remains fixed in time)

System (material volume)
and control volume at time t
(shaded region)

System at time $t + \Delta t$
(hatched region)

V_1

V_2

I

II

(1)

(2)

Inflow during Δt

Outflow during Δt

At time t: Sys = CV
At time $t + \Delta t$: Sys = CV − I + II
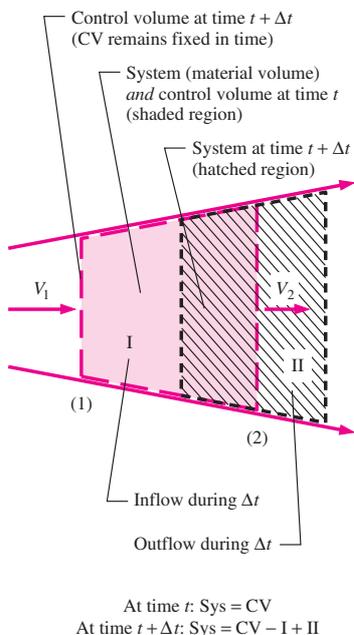
FIGURE 4–54
A moving *system* (hatched region) and
a fixed *control volume* (shaded region)
in a diverging portion of a flow field at
times t and $t + \Delta t$. The upper and lower
bounds are streamlines of the flow.

this motion is designated as section I (part of the CV), and the new region covered by the system is designated as section II (not part of the CV). Therefore, at time $t + \Delta t$, the system consists of the same fluid, but it occupies the region CV − I + II. The control volume is fixed in space, and thus it remains as the shaded region marked CV at all times.

Let *B* represent any **extensive property** (such as mass, energy, or momentum), and let $b = B/m$ represent the corresponding **intensive property.** Noting that extensive properties are additive, the extensive property *B* of the system at times t and $t + \Delta t$ can be expressed as

$$B_{\text{sys}, t} = B_{\text{CV}, t} \qquad \text{(the system and CV concide at time } t\text{)}$$

$$B_{\text{sys}, t+\Delta t} = B_{\text{CV}, t+\Delta t} - B_{\text{I}, t+\Delta t} + B_{\text{II}, t+\Delta t}$$

Subtracting the first equation from the second one and dividing by Δt gives

$$\frac{B_{\text{sys}, t+\Delta t} - B_{\text{sys}, t}}{\Delta t} = \frac{B_{\text{CV}, t+\Delta t} - B_{\text{CV}, t}}{\Delta t} - \frac{B_{\text{I}, t+\Delta t}}{\Delta t} + \frac{B_{\text{II}, t+\Delta t}}{\Delta t}$$

Taking the limit as $\Delta t \to 0$, and using the definition of derivative, we get

$$\frac{dB_{\text{sys}}}{dt} = \frac{dB_{\text{CV}}}{dt} - \dot{B}_{\text{in}} + \dot{B}_{\text{out}} \qquad \text{(4–38)}$$

or

$$\frac{dB_{\text{sys}}}{dt} = \frac{dB_{\text{CV}}}{dt} - b_1\rho_1 V_1 A_1 + b_2\rho_2 V_2 A_2$$

since

$$B_{\text{I}, t+\Delta t} = b_1 m_{\text{I}, t+\Delta t} = b_1\rho_1 V_{\text{I}, t+\Delta t} = b_1\rho_1 V_1 \, \Delta t \, A_1$$

$$B_{\text{II}, t+\Delta t} = b_2 m_{\text{II}, t+\Delta t} = b_2\rho_2 V_{\text{II}, t+\Delta t} = b_2\rho_2 V_2 \, \Delta t \, A_2$$

and

$$\dot{B}_{\text{in}} = \dot{B}_{\text{I}} = \lim_{\Delta t \to 0} \frac{B_{\text{I}, t+\Delta t}}{\Delta t} = \lim_{\Delta t \to 0} \frac{b_1\rho_1 V_1 \, \Delta t \, A_1}{\Delta t} = b_1\rho_1 V_1 \, A_1$$

$$\dot{B}_{\text{out}} = \dot{B}_{\text{II}} = \lim_{\Delta t \to 0} \frac{B_{\text{II}, t+\Delta t}}{\Delta t} = \lim_{\Delta t \to 0} \frac{b_2\rho_2 V_2 \, \Delta t \, A_2}{\Delta t} = b_2\rho_2 V_2 \, A_2$$

where A_1 and A_2 are the cross-sectional areas at locations 1 and 2. Equation 4–38 states that *the time rate of change of the property B of the system is equal to the time rate of change of B of the control volume plus the net flux of B out of the control volume by mass crossing the control surface*. This is the desired relation since it relates the change of a property of a system to the change of that property for a control volume. Note that Eq. 4–38 applies at any instant in time, where it is assumed that the system and the control volume occupy the same space at that particular instant in time.

The influx $\dot{B}_{\text{in}}$ and outflux $\dot{B}_{\text{out}}$ of the property *B* in this case are easy to determine since there is only one inlet and one outlet, and the velocities are normal to the surfaces at sections (1) and (2). In general, however, we may have several inlet and outlet ports, and the velocity may not be normal to the control surface at the point of entry. Also, the velocity may not be uniform. To generalize the process, we consider a differential surface area dA on the control surface and denote its **unit outer normal** by $\vec{n}$. The flow rate

of property b through dA is $\rho b \vec{V} \cdot \vec{n} \, dA$ since the dot product $\vec{V} \cdot \vec{n}$ gives the normal component of the velocity. Then the net rate of outflow through the entire control surface is determined by integration to be (Fig. 4–55)

$$\dot{B}_{net} = \dot{B}_{out} - \dot{B}_{in} = \int_{CS} \rho b \vec{V} \cdot \vec{n} \, dA \quad \text{(inflow if negative)} \tag{4–39}$$

An important aspect of this relation is that it automatically subtracts the inflow from the outflow, as explained next. The dot product of the velocity vector at a point on the control surface and the outer normal at that point is $\vec{V} \cdot \vec{n} = |\vec{V}||\vec{n}| \cos \theta = |\vec{V}| \cos \theta$, where θ is the angle between the velocity vector and the outer normal, as shown in Fig. 4–56. For $\theta < 90°$, we have $\cos \theta > 0$ and thus $\vec{V} \cdot \vec{n} > 0$ for outflow of mass from the control volume, and for $\theta > 90°$, we have $\cos \theta < 0$ and thus $\vec{V} \cdot \vec{n} < 0$ for inflow of mass into the control volume. Therefore, the differential quantity $\rho b \vec{V} \cdot \vec{n} \, dA$ is positive for mass flowing out of the control volume, and negative for mass flowing into the control volume, and its integral over the entire control surface gives the rate of net outflow of the property B by mass.

The properties within the control volume may vary with position, in general. In such a case, the total amount of property B within the control volume must be determined by integration:

$$B_{CV} = \int_{CV} \rho b \, dV \tag{4–40}$$

The term dB_{CV}/dt in Eq. 4–38 is thus equal to $\dfrac{d}{dt} \int_{CV} \rho b \, dV$, and represents the time rate of change of the property B content of the control volume. A positive value for dB_{CV}/dt indicates an increase in the B content, and a negative value indicates a decrease. Substituting Eqs. 4–39 and 4–40 into Eq. 4–38 yields the Reynolds transport theorem, also known as the *system-to-control-volume transformation* for a fixed control volume:

RTT, fixed CV:
$$\frac{dB_{sys}}{dt} = \frac{d}{dt} \int_{CV} \rho b \, dV + \int_{CS} \rho b \vec{V} \cdot \vec{n} \, dA \tag{4–41}$$

Since the control volume is not moving or deforming with time, the time derivative on the right-hand side can be moved inside the integral, since the domain of integration does not change with time. (In other words, it is irrelevant whether we differentiate or integrate first.) But the time derivative in that case must be expressed as a *partial* derivative ($\partial/\partial t$) since density and the quantity b may depend on the position within the control volume. Thus, an alternate form of the Reynolds transport theorem for a fixed control volume is

Alternate RTT, fixed CV:
$$\frac{dB_{sys}}{dt} = \int_{CV} \frac{\partial}{\partial t} (\rho b) \, dV + \int_{CS} \rho b \vec{V} \cdot \vec{n} \, dA \tag{4–42}$$

Equation 4–41 was derived for a *fixed* control volume. However, many practical systems such as turbine and propeller blades involve nonfixed control volumes. Fortunately, Eq. 4–41 is also valid for *moving* and/or *deforming* control volumes provided that the absolute fluid velocity $\vec{V}$ in the last term be replaced by the **relative velocity** $\vec{V}_r$,
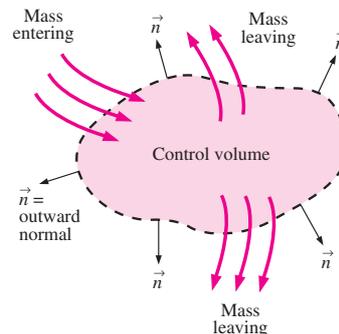
$$\dot{B}_{net} = \dot{B}_{out} - \dot{B}_{in} = \int_{CS} \rho b \vec{V} \cdot \vec{n} \, dA$$

FIGURE 4–55
The integral of $b\rho \vec{V} \cdot \vec{n} \, dA$ over the control surface gives the net amount of the property B flowing out of the control volume (into the control volume if it is negative) per unit time.
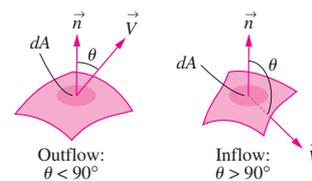
$\vec{V} \cdot \vec{n} = |\vec{V}||\vec{n}| \cos \theta = V \cos \theta$
If $\theta < 90°$, then $\cos \theta > 0$ (outflow).
If $\theta > 90°$, then $\cos \theta < 0$ (inflow).
If $\theta = 90°$, then $\cos \theta = 0$ (no flow).

FIGURE 4–56
Outflow and inflow of mass across the differential area of a control surface.
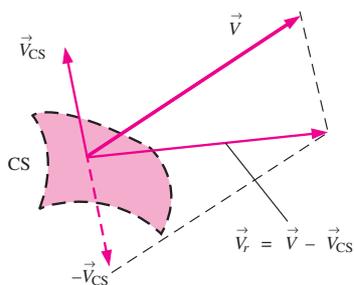
FIGURE 4–57
Relative velocity crossing a control surface is found by vector addition of the absolute velocity of the fluid and the negative of the local velocity of the control surface.

Relative velocity:
$$\vec{V}_r = \vec{V} - \vec{V}_{CS} \tag{4–43}$$

where $\vec{V}_{CS}$ is the local velocity of the control surface (Fig. 4–57). The most general form of the Reynolds transport theorem is thus

RTT, nonfixed CV:
$$\frac{dB_{sys}}{dt} = \frac{d}{dt} \int_{CV} \rho b \, dV + \int_{CS} \rho b \vec{V}_r \cdot \vec{n} \, dA \tag{4–44}$$

Note that for a control volume that moves and/or deforms with time, the time derivative must be applied *after* integration, as in Eq. 4–44. As a simple example of a moving control volume, consider a toy car moving at a constant absolute velocity $\vec{V}_{car} = 10$ km/h to the right. A high-speed jet of water (absolute velocity $= \vec{V}_{jet} = 25$ km/h to the right) strikes the back of the car and propels it (Fig. 4–58). If we draw a control volume around the car, the relative velocity is $\vec{V}_r = 25 - 10 = 15$ km/h to the right. This represents the velocity at which an observer moving with the control volume (moving with the car) would observe the fluid crossing the control surface. In other words, $\vec{V}_r$ is the fluid velocity expressed relative to a coordinate system moving *with* the control volume.

Finally, by application of the Leibnitz theorem, it can be shown that the Reynolds transport theorem for a general moving and/or deforming control volume (Eq. 4–44) is equivalent to the form given by Eq. 4–42, which is repeated here:

Alternate RTT, nonfixed CV:
$$\frac{dB_{sys}}{dt} = \int_{CV} \frac{\partial}{\partial t}(\rho b) \, dV + \int_{CS} \rho b \vec{V} \cdot \vec{n} \, dA \tag{4–45}$$

In contrast to Eq. 4–44, the velocity vector $\vec{V}$ in Eq. 4–45 must be taken as the *absolute* velocity (as viewed from a fixed reference frame) in order to apply to a nonfixed control volume.

During steady flow, the amount of the property B within the control volume remains constant in time, and thus the time derivative in Eq. 4–44 becomes zero. Then the Reynolds transport theorem reduces to

RTT, steady flow:
$$\frac{dB_{sys}}{dt} = \int_{CS} \rho b \vec{V}_r \cdot \vec{n} \, dA \tag{4–46}$$

Note that unlike the control volume, the property B content of the system may still change with time during a steady process. But in this case the change must be equal to the net property transported by mass across the control surface (an advective rather than an unsteady effect).

In most practical engineering applications of the RTT, fluid crosses the boundary of the control volume at a finite number of well-defined inlets and outlets (Fig. 4–59). In such cases, it is convenient to cut the control surface directly across each inlet and outlet and replace the surface integral in Eq. 4–44 with approximate algebraic expressions at each inlet and outlet based on the *average* values of fluid properties crossing the boundary. We define ρ_{avg}, b_{avg}, and $V_{r,\,avg}$ as the average values of ρ, b, and V_r, respectively, across an inlet or outlet of cross-sectional area A [e.g., $b_{avg} = (1/A) \int_A b \, dA$]. The

Absolute reference frame:

Control volume

Relative reference frame:
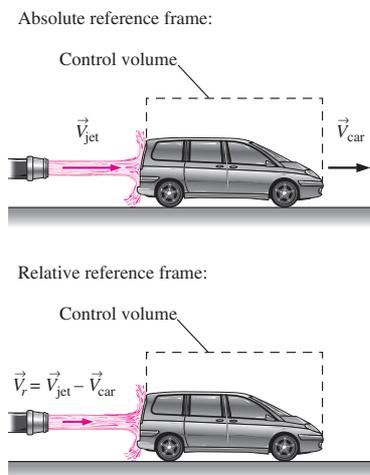
Control volume

FIGURE 4–58
Reynolds transport theorem applied to a control volume moving at constant velocity.

surface integrals in the RTT (Eq. 4–44), when applied over an inlet or outlet of cross-sectional area A, are then *approximated* by pulling property b out of the surface integral and replacing it with its average. This yields

$$\int_A \rho b \vec{V}_r \cdot \vec{n} \, dA \cong b_{avg} \int_A \rho \vec{V}_r \cdot \vec{n} \, dA = b_{avg} \dot{m}_r$$

where $\dot{m}_r$ is the mass flow rate through the inlet or outlet relative to the (moving) control surface. The approximation in this equation is exact when property b is uniform over cross-sectional area A. Equation 4–44 thus becomes

$$\frac{dB_{sys}}{dt} = \frac{d}{dt} \int_{CV} \rho b \, d\mathcal{V} + \sum_{out} \underbrace{\dot{m}_r b_{avg}}_{\text{for each outlet}} - \sum_{in} \underbrace{\dot{m}_r b_{avg}}_{\text{for each inlet}} \qquad (4\text{–}47)$$

In some applications, we may wish to rewrite Eq. 4–47 in terms of volume (rather than mass) flow rate. In such cases, we make a further approximation that $\dot{m}_r \approx \rho_{avg} \dot{\mathcal{V}}_r = \rho_{avg} V_{r,\,avg} A$. This approximation is exact when fluid density ρ is uniform over A. Equation 4–47 then reduces to

Approximate RTT for well-defined inlets and outlets:

$$\frac{dB_{sys}}{dt} = \frac{d}{dt} \int_{CV} \rho b \, d\mathcal{V} + \sum_{out} \underbrace{\rho_{avg} b_{avg} V_{r,\,avg} A}_{\text{for each outlet}} - \sum_{in} \underbrace{\rho_{avg} b_{avg} V_{r,avg} A}_{\text{for each inlet}} \qquad (4\text{–}48)$$

Note that these approximations simplify the analysis greatly but may not always be accurate, especially in cases where the velocity distribution across the inlet or outlet is not very uniform (e.g., pipe flows; Fig. 4–59). In particular, the control surface integral of Eq. 4–45 becomes *nonlinear* when property b contains a velocity term (e.g., when applying RTT to the linear momentum equation, $b = \vec{V}$), and the approximation of Eq. 4–48 leads to errors. Fortunately we can eliminate the errors by including *correction factors* in Eq. 4–48, as discussed in Chaps. 5 and 6.

Equations 4–47 and 4–48 apply to fixed *or* moving control volumes, but as discussed previously, the *relative velocity* must be used for the case of a nonfixed control volume. In Eq. 4–47 for example, the mass flow rate $\dot{m}_r$ is relative to the (moving) control surface, hence the r subscript.

*Alternate Derivation of the Reynolds Transport Theorem

A more elegant mathematical derivation of the Reynolds transport theorem is possible through use of the **Leibnitz theorem** (see Kundu, 1990). You are probably familiar with the one-dimensional version of this theorem, which allows you to differentiate an integral whose limits of integration are functions of the variable with which you need to differentiate (Fig. 4–60):

One-dimensional Leibnitz theorem:

$$\frac{d}{dt} \int_{x=a(t)}^{x=b(t)} G(x,\,t)\,dx = \int_a^b \frac{\partial G}{\partial t}\,dx + \frac{db}{dt}\,G(b,\,t) - \frac{da}{dt}\,G(a,\,t) \qquad (4\text{–}49)$$

---

* This section may be omitted without loss of continuity.
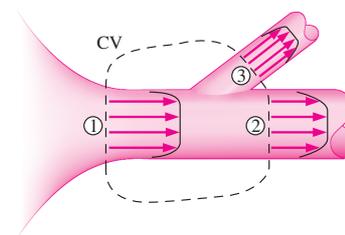
FIGURE 4–59
An example control volume in which there is one well-defined inlet (1) and two well-defined outlets (2 and 3). In such cases, the control surface integral in the RTT can be more conveniently written in terms of the average values of fluid properties crossing each inlet and outlet.
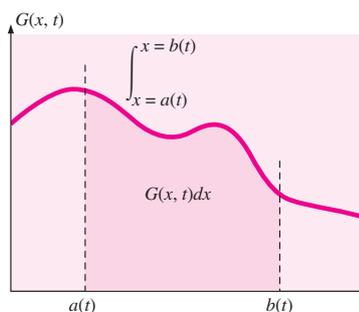
FIGURE 4–60
The *one-dimensional Leibnitz theorem* is required when calculating the time derivative of an integral (with respect to x) for which the limits of the integral are functions of time.

The Leibnitz theorem takes into account the change of limits $a(t)$ and $b(t)$ with respect to time, as well as the unsteady changes of integrand $G(x, t)$ with time.

EXAMPLE 4–10   **One-Dimensional Leibnitz Integration**

Reduce the following expression as far as possible:

$$F(t) = \frac{d}{dt} \int_{x=0}^{x=Ct} e^{-x^2} \, dx \qquad (1)$$

SOLUTION $F(t)$ is to be evaluated from the given expression.
Analysis   We could try integrating first and then differentiating, but since Eq. 1 is of the form of Eq. 4–49, we use the one-dimensional Leibnitz theorem. Here, $G(x, t) = e^{-x^2}$ (G is not a function of time in this simple example). The limits of integration are $a(t) = 0$ and $b(t) = Ct$. Thus,

$$F(t) = \int_a^b \underbrace{\frac{\partial G}{\partial t}}_{0} \, dx + \frac{db}{dt} \underbrace{G(b, t)}_{e^{-b^2}} - \underbrace{\frac{da}{dt}}_{0} G(a, t) \quad \rightarrow \quad \boxed{F(t) = Ce^{-C^2t^2}} \qquad (2)$$

(with $\frac{db}{dt} = C$)

Discussion   You are welcome to try to obtain the same solution without using the Leibnitz theorem.

In three dimensions, the Leibnitz theorem for a *volume* integral is

Three-dimensional Leibnitz theorem:

$$\frac{d}{dt} \int_{V(t)} G(x, y, z, t) \, dV = \int_{V(t)} \frac{\partial G}{\partial t} \, dV + \int_{A(t)} G\vec{V}_A \cdot \vec{n} \, dA \qquad (4\text{–}50)$$

where $V(t)$ is a moving and/or deforming volume (a function of time), $A(t)$ is its surface (boundary), and $\vec{V}_A$ is the absolute velocity of this (moving) surface (Fig. 4–61). Equation 4–50 is valid for *any* volume, moving and/or deforming arbitrarily in space and time. For consistency with the previous analyses, we set integrand G to ρb for application to fluid flow,

Three-dimensional Leibnitz theorem applied to fluid flow:

$$\frac{d}{dt} \int_{V(t)} \rho b \, dV = \int_{V(t)} \frac{\partial}{\partial t} (\rho b) \, dV + \int_{A(t)} \rho b \vec{V}_A \cdot \vec{n} \, dA \qquad (4\text{–}51)$$

If we apply the Leibnitz theorem to the special case of a **material volume** (a system of fixed identity moving with the fluid flow), then $\vec{V}_A = \vec{V}$ everywhere on the material surface since it moves *with* the fluid. Here $\vec{V}$ is the local fluid velocity, and Eq. 4–51 becomes

Leibnitz theorem applied to a material volume:

$$\frac{d}{dt} \int_{V(t)} \rho b \, dV = \frac{dB_{sys}}{dt} = \int_{V(t)} \frac{\partial}{\partial t} (\rho b) \, dV + \int_{A(t)} \rho b \vec{V} \cdot \vec{n} \, dA \qquad (4\text{–}52)$$

Equation 4–52 is valid at any instant in time t. We define our control volume such that at this time t, the control volume and the system occupy the same space; in other words, they are *coincident*. At some later time $t + \Delta t$, the system has moved and deformed with the flow, but the control volume
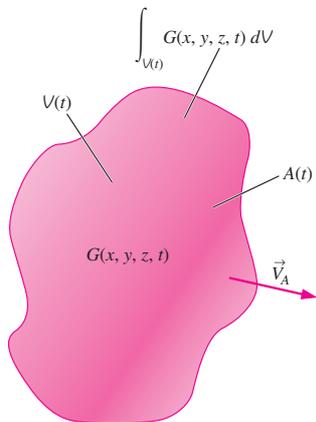
FIGURE 4–61
The *three-dimensional Leibnitz theorem* is required when calculating the time derivative of a volume integral for which the volume itself moves and/or deforms with time. It turns out that the three-dimensional form of the Leibnitz theorem can be used in an alternative derivation of the Reynolds transport theorem.

may have moved and deformed differently (Fig. 4–62). The key, however, is that *at time t, the system (material volume) and control volume are one and the same.* Thus, the volume integral on the right-hand side of Eq. 4–52 can be evaluated over the *control volume* at time *t*, and the surface integral can be evaluated over the *control surface* at time *t*. Hence,

General RTT, nonfixed CV: $\dfrac{dB_{sys}}{dt} = \displaystyle\int_{CV} \dfrac{\partial}{\partial t}(\rho b)\, dV + \int_{CS} \rho b \vec{V} \cdot \vec{n}\, dA$ **(4–53)**

This expression is identical to that of Eq. 4–45 and is valid for an arbitrarily shaped, moving, and/or deforming control volume at time *t*. Keep in mind that $\vec{V}$ in Eq. 4–53 is the *absolute* fluid velocity.

FIGURE 4–62
The material volume (system) and control volume occupy the same space at time *t* (the blue shaded area), but move and deform differently. At a later time they are *not* coincident.

EXAMPLE 4–11   **Reynolds Transport Theorem in Terms of Relative Velocity**

Beginning with the Leibnitz theorem and the general Reynolds transport theorem for an arbitrarily moving and deforming control volume, Eq. 4–53, prove that Eq. 4–44 is valid.

SOLUTION   Equation 4–44 is to be proven.
Analysis   The general three-dimensional version of the Leibnitz theorem, Eq. 4–50, applies to *any* volume. We choose to apply it to the control volume of interest, which can be moving and/or deforming differently than the material volume (Fig. 4–62). Setting *G* to ρb, Eq. 4–50 becomes

$$\frac{d}{dt}\int_{CV}\rho b\, dV = \int_{CV}\frac{\partial}{\partial t}(\rho b)\, dV + \int_{CS}\rho b \vec{V}_{CS}\cdot\vec{n}\, dA \tag{1}$$

We solve Eq. 4–53 for the control volume integral,

$$\int_{CV}\frac{\partial}{\partial t}(\rho b)\, dV = \frac{dB_{sys}}{dt} - \int_{CS}\rho b \vec{V}\cdot\vec{n}\, dA \tag{2}$$

Substituting Eq. 2 into Eq. 1, we get

$$\frac{d}{dt}\int_{CV}\rho b\, dV = \frac{dB_{sys}}{dt} - \int_{CS}\rho b \vec{V}\cdot\vec{n}\, dA + \int_{CS}\rho b \vec{V}_{CS}\cdot\vec{n}\, dA \tag{3}$$

Combining the last two terms and rearranging,

$$\frac{dB_{sys}}{dt} = \frac{d}{dt}\int_{CV}\rho b\, dV + \int_{CS}\rho b(\vec{V}-\vec{V}_{CS})\cdot\vec{n}\, dA \tag{4}$$

But recall that the relative velocity is defined by Eq. 4–43. Thus,

RTT in terms of relative velocity: $\dfrac{dB_{sys}}{dt} = \dfrac{d}{dt}\displaystyle\int_{CV}\rho b\, dV + \int_{CS}\rho b \vec{V}_r \cdot \vec{n}\, dA$ **(5)**

Discussion   Equation 5 is indeed identical to Eq. 4–44, and the power and elegance of the Leibnitz theorem are demonstrated.

Relationship between Material Derivative and RTT

You may have noticed a similarity or analogy between the material derivative discussed in Section 4–1 and the Reynolds transport theorem discussed here. In fact, both analyses represent methods to transform from fundamentally

156
FLUID MECHANICS
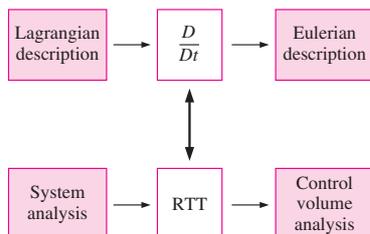
FIGURE 4–63
The Reynolds transport theorem for finite volumes (integral analysis) is analogous to the material derivative for infinitesimal volumes (differential analysis). In both cases, we transform from a Lagrangian or system viewpoint to an Eulerian or control volume viewpoint.

Lagrangian concepts to Eulerian interpretations of those concepts. While the Reynolds transport theorem deals with finite-size control volumes and the material derivative deals with infinitesimal fluid particles, the same fundamental physical interpretation applies to both (Fig. 4–63). In fact, the Reynolds transport theorem can be thought of as the integral counterpart of the material derivative. In either case, the total rate of change of some property following an identified portion of fluid consists of two parts: There is a local or unsteady part that accounts for changes in the flow field with time (compare the first term on the right-hand side of Eq. 4-12 to that of Eq. 4-45). There is also an advective part that accounts for the movement of fluid from one region of the flow to another (compare the second term on the right-hand sides of Eqs. 4-12 and 4-45).

Just as the material derivative can be applied to any fluid property, scalar or vector, the Reynolds transport theorem can be applied to any scalar or vector property as well. In Chaps. 5 and 6, we apply the Reynolds transport theorem to conservation of mass, energy, momentum, and angular momentum by choosing parameter B to be mass, energy, momentum, and angular momentum, respectively. In this fashion we can easily convert from the fundamental system conservation laws (Lagrangian viewpoint) to forms that are valid and useful in a control volume analysis (Eulerian viewpoint).

SUMMARY

Fluid kinematics is concerned with describing fluid motion, without necessarily analyzing the forces responsible for such motion. There are two fundamental descriptions of fluid motion—*Lagrangian* and *Eulerian*. In a Lagrangian description, we follow individual fluid particles or collections of fluid particles, while in the Eulerian description, we define a *control volume* through which fluid flows in and out. We transform equations of motion from Lagrangian to Eulerian through use of the *material derivative* for infinitesimal fluid particles and through use of the *Reynolds transport theorem* (*RTT*) for systems of finite volume. For some extensive property B or its corresponding intensive property b,

Material derivative:
$$\frac{Db}{Dt} = \frac{\partial b}{\partial t} + (\vec{V} \cdot \vec{\nabla})b$$

General RTT, nonfixed CV:
$$\frac{dB_{sys}}{dt} = \int_{CV} \frac{\partial}{\partial t}(\rho b)\,dV + \int_{CS} \rho b \vec{V} \cdot \vec{n}\,dA$$

In both equations, the total change of the property following a fluid particle or following a system is composed of two parts: a *local* (unsteady) part and an *advective* (movement) part.

There are various ways to visualize and analyze flow fields—*streamlines*, *streaklines*, *pathlines*, *timelines*, *surface imaging*, *shadowgraphy*, *schlieren imaging*, *profile plots*, *vector plots*, and *contour plots*. We define each of these and provide examples in this chapter. In general unsteady flow, streamlines, streaklines, and pathlines differ, but *in steady flow, streamlines, streaklines, and pathlines are coincident*.

Four fundamental rates of motion (*deformation rates*) are required to fully describe the kinematics of a fluid flow: *velocity* (rate of translation), *angular velocity* (rate of rotation), *linear strain rate*, and *shear strain rate*. *Vorticity* is a property of fluid flows that indicates the *rotationality* of fluid particles.

Vorticity vector: $\vec{\zeta} = \vec{\nabla} \times \vec{V} = \text{curl}(\vec{V}) = 2\vec{\omega}$

A region of flow is *irrotational* if the vorticity is zero in that region.

The concepts learned in this chapter are used repeatedly throughout the rest of the book. We use the RTT to transform the conservation laws from closed systems to control volumes in Chaps. 5 and 6, and again in Chap. 9 in the derivation of the differential equations of fluid motion. The role of vorticity and irrotationality is revisited in greater detail in Chap. 10 where we show that the irrotationality approximation leads to greatly reduced complexity in the solution of fluid flows. Finally, we use various types of flow visualization and data plots to describe the kinematics of example flow fields in nearly every chapter of this book.

APPLICATION SPOTLIGHT ■ Fluidic Actuators

Guest Author: Ganesh Raman,
Illinois Institute of Technology

Fluidic actuators are devices that use fluid logic circuits to produce oscilla-
tory velocity or pressure perturbations in jets and shear layers for delaying
separation, enhancing mixing, and suppressing noise. Fluidic actuators are
potentially useful for shear flow control applications for many reasons: they
have no moving parts; they can produce perturbations that are controllable in
frequency, amplitude, and phase; they can operate in harsh thermal environ-
ments and are not susceptible to electromagnetic interference; and they are
easy to integrate into a functioning device. Although fluidics technology has
been around for many years, recent advances in miniaturization and micro-
fabrication have made them very attractive candidates for practical use. The
fluidic actuator produces a self-sustaining oscillatory flow using the princi-
ples of wall attachment and backflow that occur within miniature passages of
the device.

Figure 4–64 demonstrates the application of a fluidic actuator for jet thrust
vectoring. Fluidic thrust vectoring is important for future aircraft designs,
since they can improve maneuverability without the complexity of additional
surfaces near the nozzle exhaust. In the three images of Fig. 4–64, the pri-
mary jet exhausts from right to left and a single fluidic actuator is located at
the top. Figure 4–64a shows the unperturbed jet. Figures 4–64b and c show
the vectoring effect at two fluidic actuation levels. Changes to the primary jet
are characterized using particle image velocimetry (PIV). A simplified expla-
nation is as follows: In this technique tracer particles are introduced into the
flow and illuminated by a thin laser light sheet that is pulsed to freeze parti-
cle motion. Laser light scattered by the particles is recorded at two instances
in time using a digital camera. Using a spatial cross correlation, the local dis-
placement vector is obtained. The results indicate that there exists the poten-
tial for integrating multiple fluidic subelements into aircraft components for
improved performance.

Figure 4–64 is actually a combination vector plot and contour plot. Veloc-
ity vectors are superimposed on contour plots of velocity magnitude (speed).
The white regions represent high speeds, and the dark regions represent low
speeds.

References

Raman, G., Packiarajan, S., Papadopoulos, G., Weissman, C., and Raghu, S., "Jet
Thrust Vectoring Using a Miniature Fluidic Oscillator," ASME FEDSM 2001-
18057, 2001.
Raman, G., Raghu, S., and Bencic, T. J., "Cavity Resonance Suppression Using
Miniature Fluidic Oscillators," AIAA Paper 99-1900, 1999.
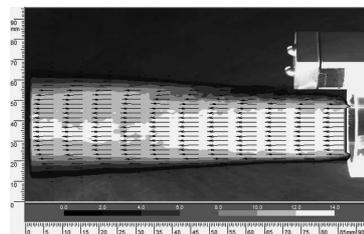
(a)
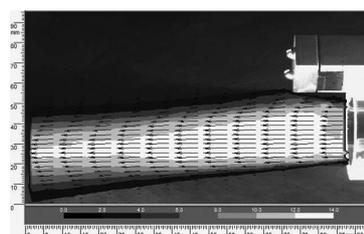
(b)
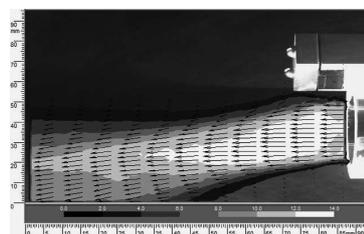
(c)

FIGURE 4–64

Time-averaged mean velocity field of
a fluidic actuator jet. Results are from
150 PIV realizations, overlaid on an
image of the seeded flow. Every
seventh and second velocity vector is
shown in the horizontal and vertical
directions, respectively. The contour
levels denote the magnitude of the
velocity field in m/s. (a) No actuation;
(b) single actuator operating at 3 psig;
(c) single actuator operating at 9 psig.

*Courtesy Ganesh Raman, Illinois Institute of
Technology. Used by permission.*

REFERENCES AND SUGGESTED READING

1. R. J. Adrian. "Particle-Imaging Technique for Experimental Fluid Mechanics," *Annual Reviews in Fluid Mechanics*, 23, pp. 261–304, 1991.

2. J. M. Cimbala, H. Nagib, and A. Roshko. "Large Structure in the Far Wakes of Two-Dimensional Bluff Bodies," *Journal of Fluid Mechanics,* 190, pp. 265–298, 1988.

3. R. J. Heinsohn and J. M. Cimbala. *Indoor Air Quality Engineering*. New York: Marcel-Dekker, 2003.

4. P. K. Kundu. *Fluid Mechanics*. San Diego, CA: Academic Press, 1990.

5. W. Merzkirch. *Flow Visualization*, 2nd ed. Orlando, FL: Academic Press, 1987.

6. G. S. Settles. *Schlieren and Shadowgraph Techniques: Visualizing Phenomena in Transparent Media*. Heidelberg: Springer-Verlag, 2001.

7. M. Van Dyke. *An Album of Fluid Motion*. Stanford, CA: The Parabolic Press, 1982.

8. F. M. White. *Viscous Fluid Flow*, 2nd ed. New York: McGraw-Hill, 1991.

PROBLEMS*

Introductory Problems

4–1C What does the word *kinematics* mean? Explain what the study of *fluid kinematics* involves.

4–2 Consider steady flow of water through an axisymmetric garden hose nozzle (Fig. P4–2). Along the centerline of the nozzle, the water speed increases from $u_{entrance}$ to u_{exit} as sketched. Measurements reveal that the centerline water speed increases parabolically through the nozzle. Write an equation for centerline speed $u(x)$, based on the parameters given here, from $x = 0$ to $x = L$.
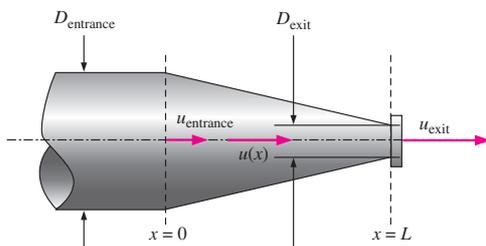
FIGURE P4–2

* Problems designated by a "C" are concept questions, and students are encouraged to answer them all. Problems designated by an "E" are in English units, and the SI users can ignore them. Problems with the ⊛ icon are solved using EES, and complete solutions together with parametric studies are included on the enclosed DVD. Problems with the 🖳 icon are comprehensive in nature and are intended to be solved with a computer, preferably using the EES software that accompanies this text.

4–3 Consider the following steady, two-dimensional velocity field:

$$\vec{V} = (u, v) = (0.5 + 1.2x)\vec{i} + (-2.0 - 1.2y)\vec{j}$$

Is there a stagnation point in this flow field? If so, where is it?
Answer: x = −0.417, y = −1.67

4–4 Consider the following steady, two-dimensional velocity field:

$$\vec{V} = (u, v) = (a^2 - (b - cx)^2)\vec{i} + (-2cby + 2c^2xy)\vec{j}$$

Is there a stagnation point in this flow field? If so, where is it?

Lagrangian and Eulerian Descriptions

4–5C What is the *Lagrangian description* of fluid motion?

4–6C Is the Lagrangian method of fluid flow analysis more similar to study of a system or a control volume? Explain.

4–7C What is the *Eulerian description* of fluid motion? How does it differ from the Lagrangian description?

4–8C A stationary probe is placed in a fluid flow and measures pressure and temperature as functions of time at one
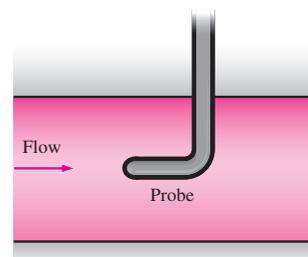
FIGURE P4–8C

location in the flow (Fig. P4–8C). Is this a Lagrangian or an Eulerian measurement? Explain.

4–9C A tiny neutrally buoyant electronic pressure probe is released into the inlet pipe of a water pump and transmits 2000 pressure readings per second as it passes through the pump. Is this a Lagrangian or an Eulerian measurement? Explain.

4–10C A weather balloon is launched into the atmosphere by meteorologists. When the balloon reaches an altitude where it is neutrally buoyant, it transmits information about weather conditions to monitoring stations on the ground (Fig. P4–10C). Is this a Lagrangian or an Eulerian measurement? Explain.

Helium-filled
weather balloon

Transmitting
instrumentation
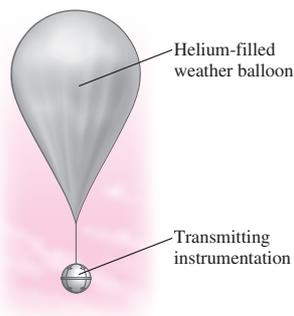
FIGURE P4–10C

4–11C A Pitot-static probe can often be seen protruding from the underside of an airplane (Fig. P4–11C). As the airplane flies, the probe measures relative wind speed. Is this a Lagrangian or an Eulerian measurement? Explain.

Probe
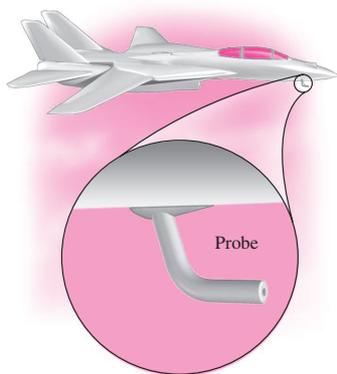
FIGURE P4–11C

4–12C Is the Eulerian method of fluid flow analysis more similar to study of a system or a control volume? Explain.

4–13C Define a *steady flow field* in the Eulerian reference frame. In such a steady flow, is it possible for a fluid particle to experience a nonzero acceleration?

4–14C List at least three other names for the material derivative, and write a brief explanation about why each name is appropriate.

4–15 Consider steady, incompressible, two-dimensional flow through a converging duct (Fig. P4–15). A simple approximate velocity field for this flow is

$$\vec{V} = (u, v) = (U_0 + bx)\vec{i} - by\vec{j}$$

where U_0 is the horizontal speed at $x = 0$. Note that this equation ignores viscous effects along the walls but is a reasonable approximation throughout the majority of the flow field. Calculate the material acceleration for fluid particles passing through this duct. Give your answer in two ways: (1) as acceleration components a_x and a_y and (2) as acceleration vector $\vec{a}$.

y
x
U_0
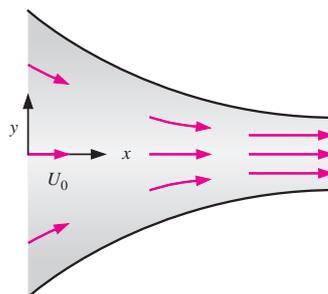
FIGURE P4–15

4–16 Converging duct flow is modeled by the steady, two-dimensional velocity field of Prob. 4–15. The pressure field is given by

$$P = P_0 - \frac{\rho}{2}\left[2U_0 bx + b^2(x^2 + y^2)\right]$$

where P_0 is the pressure at $x = 0$. Generate an expression for the rate of change of pressure *following a fluid particle*.

4–17 A steady, incompressible, two-dimensional velocity field is given by the following components in the xy-plane:

$$u = 1.1 + 2.8x + 0.65y \qquad v = 0.98 - 2.1x - 2.8y$$

Calculate the acceleration field (find expressions for acceleration components a_x and a_y), and calculate the acceleration at the point $(x, y) = (-2, 3)$.   *Answers: $a_x = -9.233$, $a_y = 14.37$*

4–18 A steady, incompressible, two-dimensional velocity field is given by the following components in the xy-plane:

$$u = 0.20 + 1.3x + 0.85y \qquad v = -0.50 + 0.95x - 1.3y$$

Calculate the acceleration field (find expressions for acceleration components a_x and a_y) and calculate the acceleration at the point $(x, y) = (1, 2)$.

4–19 For the velocity field of Prob. 4–2, calculate the fluid acceleration along the nozzle centerline as a function of x and the given parameters.

4–20 Consider steady flow of air through the diffuser portion of a wind tunnel (Fig. P4–20). Along the centerline of the diffuser, the air speed decreases from $u_{entrance}$ to u_{exit} as sketched. Measurements reveal that the centerline air speed decreases parabolically through the diffuser. Write an equation for centerline speed $u(x)$, based on the parameters given here, from $x = 0$ to $x = L$.
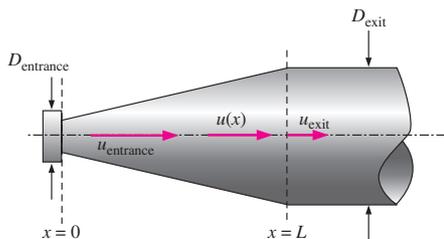
FIGURE P4–20

4–21 For the velocity field of Prob. 4–20, calculate the fluid acceleration along the diffuser centerline as a function of x and the given parameters. For $L = 2.0$ m, $u_{entrance} = 30.0$ m/s, and $u_{exit} = 5.0$ m/s, calculate the acceleration at $x = 0$ and $x = 1.0$ m. *Answers:* 0, -297 m/s^2

Flow Patterns and Flow Visualization

4–22C What is the definition of a *streamline*? What do streamlines indicate?

4–23 Converging duct flow (Fig. P4–15) is modeled by the steady, two-dimensional velocity field of Prob. 4–15. Generate an analytical expression for the flow streamlines.
Answer: $y = C/(U_0 + bx)$

4–24E Converging duct flow is modeled by the steady, two-dimensional velocity field of Prob. 4–15. For the case in which $U_0 = 5.0$ ft/s and $b = 4.6$ s^{-1}, plot several streamlines from $x = 0$ ft to 5 ft and $y = -3$ ft to 3 ft. Be sure to show the *direction* of the streamlines.

4–25C Consider the visualization of flow over a 12° cone in Fig. P4–25C. Are we seeing streamlines, streaklines, pathlines, or timelines? Explain.
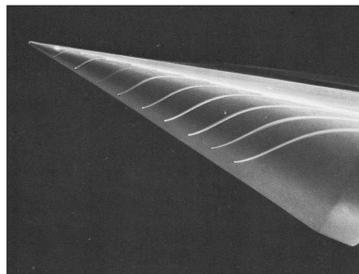
FIGURE P4–25C
Visualization of flow over a 12° cone at a 16° angle of attack at a Reynolds number of 15,000. The visualization is produced by colored fluid injected into water from ports in the body.
Courtesy ONERA. Photograph by Werlé.

4–26C What is the definition of a *pathline*? What do pathlines indicate?

4–27C What is the definition of a *streakline*? How do streaklines differ from streamlines?

4–28C Consider the visualization of flow over a 15° delta wing in Fig. P4–28C. Are we seeing streamlines, streaklines, pathlines, or timelines? Explain.
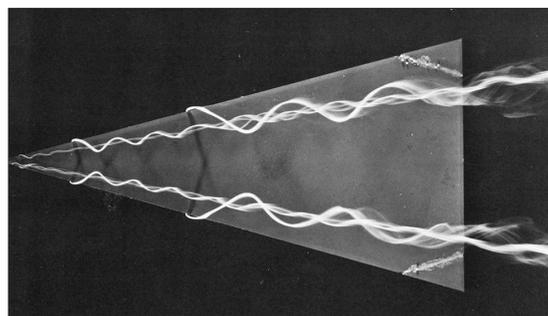
FIGURE P4–28C
Visualization of flow over a 15° delta wing at a 20° angle of attack at a Reynolds number of 20,000. The visualization is produced by colored fluid injected into water from ports on the underside of the wing.
Courtesy ONERA. Photograph by Werlé.

4–29C Consider the visualization of ground vortex flow in Fig. P4–29C. Are we seeing streamlines, streaklines, pathlines, or timelines? Explain.
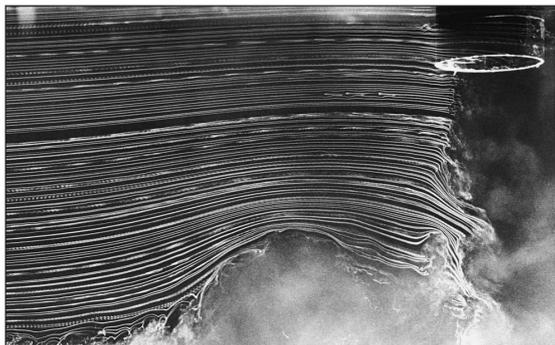
FIGURE P4–29C
Visualization of ground vortex flow. A high-speed round
air jet impinges on the ground in the presence of a free-
stream flow of air from left to right. (The ground is at the
bottom of the picture.) The portion of the jet that travels
upstream forms a recirculating flow known as a **ground
vortex.** The visualization is produced by a smoke wire
mounted vertically to the left of the field of view.
Photo by John M. Cimbala.

4–30C Consider the visualization of flow over a sphere in
Fig. P4–30C. Are we seeing streamlines, streaklines, path-
lines, or timelines? Explain.
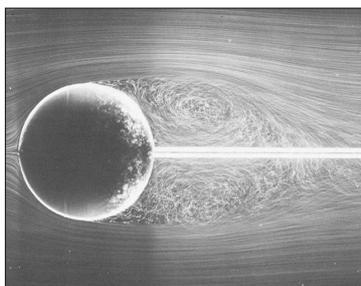
FIGURE P4–30C
Visualization of flow over a sphere at a Reynolds number
of 15,000. The visualization is produced by a time
exposure of air bubbles in water.
Courtesy ONERA. Photograph by Werlé.

4–31C What is the definition of a *timeline*? How can time-
lines be produced in a water channel? Name an application
where timelines are more useful than streaklines.

4–32C Consider a cross-sectional slice through an array of
heat exchanger tubes (Fig. P4–32C). For each desired piece
of information, choose which kind of flow visualization plot

(vector plot or contour plot) would be most appropriate, and
explain why.

(*a*) The location of maximum fluid speed is to be visualized.

(*b*) Flow separation at the rear of the tubes is to be visualized.

(*c*) The temperature field throughout the plane is to be
visualized.

(*d*) The distribution of the vorticity component normal to the
plane is to be visualized.
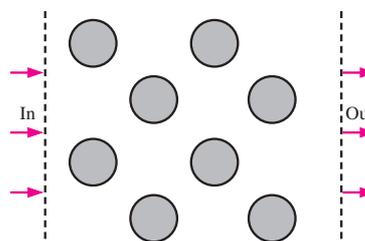
FIGURE P4–32C

4–33 Consider the following steady, incompressible, two-
dimensional velocity field:

$$\vec{V} = (u, v) = (0.5 + 1.2x)\vec{i} + (-2.0 - 1.2y)\vec{j}$$

Generate an analytical expression for the flow streamlines
and draw several streamlines in the upper-right quadrant from
$x = 0$ to 5 and $y = 0$ to 6.

4–34 Consider the steady, incompressible, two-dimensional
velocity field of Prob. 4–33. Generate a velocity vector plot
in the upper-right quadrant from $x = 0$ to 5 and $y = 0$ to 6.

4–35 Consider the steady, incompressible, two-dimensional
velocity field of Prob. 4–33. Generate a vector plot of the
acceleration field in the upper-right quadrant from $x = 0$ to 5
and $y = 0$ to 6.

4–36 A steady, incompressible, two-dimensional velocity
field is given by

$$\vec{V} = (u, v) = (1 + 2.5x + y)\vec{i} + (-0.5 - 1.5x - 2.5y)\vec{j}$$

where the *x*- and *y*-coordinates are in m and the magnitude of
velocity is in m/s.

(*a*) Determine if there are any stagnation points in this flow
field, and if so, where they are.

(*b*) Sketch velocity vectors at several locations in the upper-
right quadrant for $x = 0$ m to 4 m and $y = 0$ m to 4 m; qual-
itatively describe the flow field.

4–37 Consider the steady, incompressible, two-dimensional
velocity field of Prob. 4–36.

(*a*) Calculate the material acceleration at the point ($x = 2$ m,
$y = 3$ m).   *Answers: $a_x = 11.5$ m/s^2, $a_y = 14.0$ m/s^2*

(*b*) Sketch the material acceleration vectors at the same array
of *x*- and *y*-values as in Prob. 4–36.

4–38 The velocity field for *solid-body rotation* in the $r\theta$-plane (Fig. P4–38) is given by

$$u_r = 0 \qquad u_\theta = \omega r$$

where ω is the magnitude of the angular velocity ($\vec{\omega}$ points in the z-direction). For the case with $\omega = 1.0\ \text{s}^{-1}$, plot a contour plot of velocity magnitude (speed). Specifically, draw curves of constant speed $V = 0.5$, 1.0, 1.5, 2.0, and 2.5 m/s. Be sure to label these speeds on your plot.
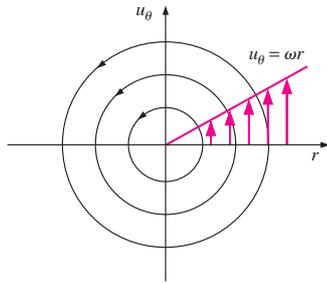
FIGURE P4–38

4–39 The velocity field for a *line vortex* in the $r\theta$-plane (Fig. P4–39) is given by

$$u_r = 0 \qquad u_\theta = \frac{K}{r}$$
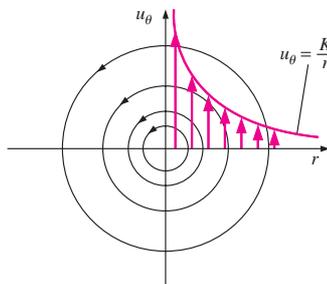
FIGURE P4–39

where K is the *line vortex strength*. For the case with $K = 1.0\ \text{m}^2/\text{s}$, plot a contour plot of velocity magnitude (speed). Specifically, draw curves of constant speed $V = 0.5$, 1.0, 1.5, 2.0, and 2.5 m/s. Be sure to label these speeds on your plot.

4–40 The velocity field for a *line source* in the $r\theta$-plane (Fig. P4–40) is given by

$$u_r = \frac{m}{2\pi r} \qquad u_\theta = 0$$

where m is the line source strength. For the case with $m/(2\pi) = 1.0\ \text{m}^2/\text{s}$, plot a contour plot of velocity magnitude (speed). Specifically, draw curves of constant speed $V = 0.5$, 1.0, 1.5, 2.0, and 2.5 m/s. Be sure to label these speeds on your plot.
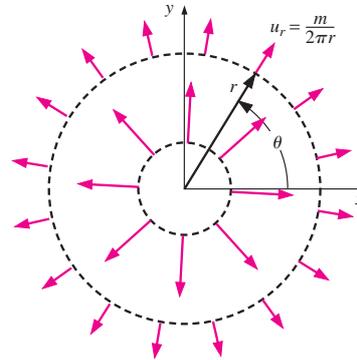
FIGURE P4–40

Motion and Deformation of Fluid Elements

4–41C Name and briefly describe the four fundamental types of motion or deformation of fluid particles.

4–42 Converging duct flow (Fig. P4–15) is modeled by the steady, two-dimensional velocity field of Prob. 4–15. Is this flow field rotational or irrotational? Show all your work. *Answer:* irrotational

4–43 Converging duct flow is modeled by the steady, two-dimensional velocity field of Prob. 4–15. A fluid particle (A) is located on the x-axis at $x = x_A$ at time $t = 0$ (Fig. P4–43). At some later time t, the fluid particle has moved downstream with the flow to some new location $x = x_{A'}$, as shown in the
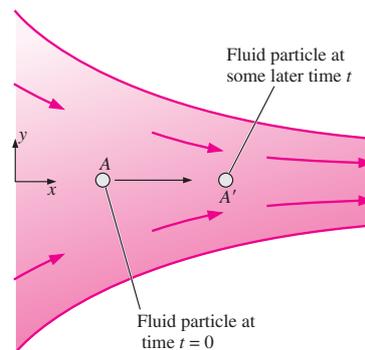
FIGURE P4–43

figure. Since the flow is symmetric about the x-axis, the fluid particle remains on the x-axis at all times. Generate an analytical expression for the x-location of the fluid particle at some arbitrary time t in terms of its initial location x_A and constants U_0 and b. In other words, develop an expression for $x_{A'}$. (Hint: We know that $u = dx_{particle}/dt$ following a fluid particle. Plug in u, separate variables, and integrate.)

4–44 Converging duct flow is modeled by the steady, two-dimensional velocity field of Prob. 4–15. Since the flow is symmetric about the x-axis, line segment AB along the x-axis remains on the axis, but stretches from length ξ to length $\xi + \Delta\xi$ as it flows along the channel centerline (Fig. P4–44). Generate an analytical expression for the change in length of the line segment, $\Delta\xi$. (Hint: Use the result of Prob. 4–43.)
Answer: $(x_B - x_A)(e^{bt} - 1)$
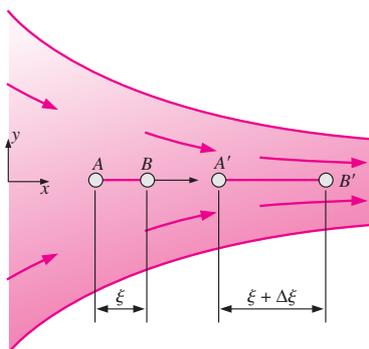
FIGURE P4–44

4–45 Using the results from Prob. 4–44 and the fundamental definition of linear strain rate (the rate of increase in length per unit length), develop an expression for the linear strain rate in the x-direction (ε_{xx}) of fluid particles located on the centerline of the channel. Compare your result to the general expression for ε_{xx} in terms of the velocity field, i.e., $\varepsilon_{xx} = \partial u/\partial x$. (Hint: Take the limit as time $t \to 0$. You may need to apply a truncated series expansion for e^{bt}.)   *Answer: b*

4–46 Converging duct flow is modeled by the steady, two-dimensional velocity field of Prob. 4–15. A fluid particle (A) is located at $x = x_A$ and $y = y_A$ at time $t = 0$ (Fig. P4–46). At some later time t, the fluid particle has moved downstream with the flow to some new location $x = x_{A'}$, $y = y_{A'}$, as shown in the figure. Generate an analytical expression for the y-location of the fluid particle at arbitrary time t in terms of its initial y-location y_A and constant b. In other words, develop an expression for $y_{A'}$. (Hint: We know that $v = dy_{particle}/dt$ following a fluid particle. Substitute the equation for v, separate variables, and integrate.)   *Answer:* $y_A e^{-bt}$
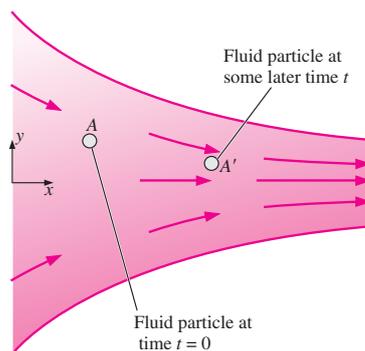
FIGURE P4–46

4–47 Converging duct flow is modeled by the steady, two-dimensional velocity field of Prob. 4–15. As vertical line segment AB moves downstream it shrinks from length η to length $\eta + \Delta\eta$ as sketched in Fig. P4–47. Generate an analytical expression for the change in length of the line segment, $\Delta\eta$. Note that the change in length, $\Delta\eta$, is *negative*. (Hint: Use the result of Prob. 4–46.)
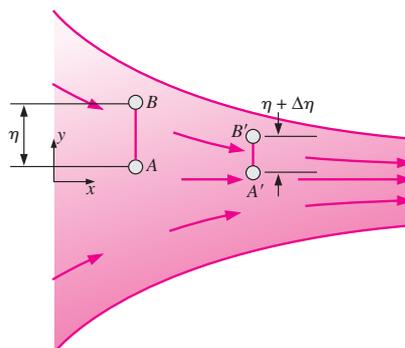
FIGURE P4–47

4–48 Using the results of Prob. 4–47 and the fundamental definition of linear strain rate (the rate of increase in length per unit length), develop an expression for the linear strain rate in the y-direction (ε_{yy}) of fluid particles moving down the channel. Compare your result to the general expression for ε_{yy} in terms of the velocity field, i.e., $\varepsilon_{yy} = \partial v/\partial y$. (Hint: Take the limit as time $t \to 0$. You may need to apply a truncated series expansion for e^{-bt}.)

4–49E Converging duct flow is modeled by the steady, two-dimensional velocity field of Prob. 4–15. For the case in which $U_0 = 5.0$ ft/s and $b = 4.6$ s^{-1}, consider an initially square fluid particle of edge dimension 0.5 ft, centered at $x = 0.5$ ft and $y = 1.0$ ft at $t = 0$ (Fig. P4–49E).

Carefully calculate and plot where the fluid particle will be and what it will look like at time $t = 0.2$ s later. Comment on the fluid particle's distortion. (Hint: Use the results of Probs. 4–43 and 4–46.)
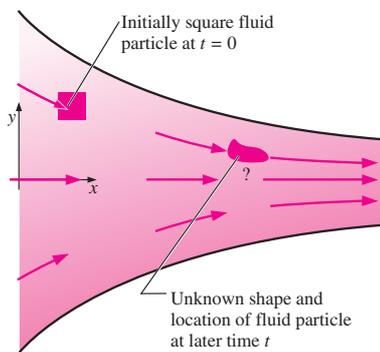
FIGURE P4–49E

4–50E Based on the results of Prob. 4–49E, verify that the converging duct flow field is indeed incompressible.

4–51 Converging duct flow is modeled by the steady, two-dimensional velocity field of Prob. 4–15. Use the equation for volumetric strain rate to verify that this flow field is incompressible.

4–52 A general equation for a steady, two-dimensional velocity field that is linear in both spatial directions (x and y) is

$$\vec{V} = (u, v) = (U + a_1x + b_1y)\vec{i} + (V + a_2x + b_2y)\vec{j}$$

where U and V and the coefficients are constants. Their dimensions are assumed to be appropriately defined. Calculate the x- and y-components of the acceleration field.

4–53 For the velocity field of Prob. 4–52, what relationship must exist between the coefficients to ensure that the flow field is incompressible?   *Answer:* $a_1 + b_2 = 0$

4–54 For the velocity field of Prob. 4–52, calculate the linear strain rates in the x- and y-directions.   *Answers:* a_1, b_2

4–55 For the velocity field of Prob. 4–52, calculate the shear strain rate in the xy-plane.

4–56 Combine your results from Probs. 4–54 and 4–55 to form the two-dimensional strain rate tensor ε_{ij} in the xy-plane,

$$\varepsilon_{ij} = \begin{pmatrix} \varepsilon_{xx} & \varepsilon_{xy} \\ \varepsilon_{yx} & \varepsilon_{yy} \end{pmatrix}$$

Under what conditions would the x- and y-axes be principal axes?   *Answer:* $b_1 + a_2 = 0$

4–57 For the velocity field of Prob. 4–52, calculate the vorticity vector. In which direction does the vorticity vector point?   *Answer:* $(a_2 - b_1)\vec{k}$

4–58 Consider steady, incompressible, two-dimensional **shear flow** for which the velocity field is

$$\vec{V} = (u, v) = (a + by)\vec{i} + 0\vec{j}$$

where a and b are constants. Sketched in Fig. P4–58 is a small rectangular fluid particle of dimensions dx and dy at time t. The fluid particle moves and deforms with the flow such that at a later time $(t + dt)$, the particle is no longer rectangular, as also shown in the figure. The initial location of each corner of the fluid particle is labeled in Fig. P4–58. The lower-left corner is at (x, y) at time t, where the x-component of velocity is $u = a + by$. At the later time, this corner moves to $(x + u\, dt, y)$, or

$$(x + (a + by)\, dt, y)$$

(*a*) In similar fashion, calculate the location of each of the other three corners of the fluid particle at time $t + dt$.

(*b*) From the fundamental definition of *linear strain rate* (the rate of increase in length per unit length), calculate linear strain rates ε_{xx} and ε_{yy}.   *Answers:* 0, 0

(*c*) Compare your results with those obtained from the equations for ε_{xx} and ε_{yy} in Cartesian coordinates, i.e.,

$$\varepsilon_{xx} = \frac{\partial u}{\partial x} \qquad \varepsilon_{yy} = \frac{\partial v}{\partial y}$$
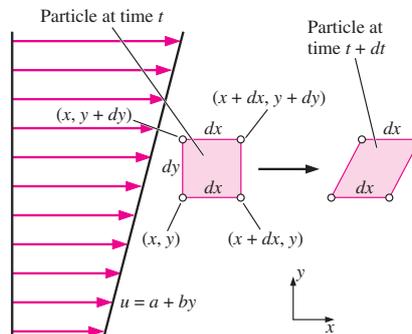
FIGURE P4–58

4–59 Use two methods to verify that the flow of Prob. 4–58 is incompressible: (*a*) by calculating the volume of the fluid particle at both times, and (*b*) by calculating the volumetric strain rate. Note that Prob. 4–58 should be completed before this problem.

4–60 Consider the steady, incompressible, two-dimensional flow field of Prob. 4–58. Using the results of Prob. 4–58(*a*), do the following:

(*a*) From the fundamental definition of *shear strain rate* (half of the rate of decrease of the angle between two initially perpendicular lines that intersect at a point), calculate shear

strain rate ε_{xy} in the xy-plane. (Hint: Use the lower edge and the left edge of the fluid particle, which intersect at 90° at the lower-left corner of the particle at the initial time.)

(b) Compare your results with those obtained from the equation for ε_{xy} in Cartesian coordinates, i.e.,

$$\varepsilon_{xy} = \frac{1}{2}\left(\frac{\partial u}{\partial y} + \frac{\partial v}{\partial x}\right)$$

Answers: (a) b/2, (b) b/2

4–61 Consider the steady, incompressible, two-dimensional flow field of Prob. 4–58. Using the results of Prob. 4–58(a), do the following:

(a) From the fundamental definition of the *rate of rotation* (average rotation rate of two initially perpendicular lines that intersect at a point), calculate the rate of rotation of the fluid particle in the xy-plane, ω_z. (Hint: Use the lower edge and the left edge of the fluid particle, which intersect at 90° at the lower-left corner of the particle at the initial time.)

(b) Compare your results with those obtained from the equation for ω_z in Cartesian coordinates, i.e.,

$$\omega_z = \frac{1}{2}\left(\frac{\partial v}{\partial x} - \frac{\partial u}{\partial y}\right)$$

Answers: (a) −b/2, (b) −b/2

4–62 From the results of Prob. 4–61,

(a) Is this flow rotational or irrotational?

(b) Calculate the z-component of vorticity for this flow field.

4–63 A two-dimensional fluid element of dimensions dx and dy translates and distorts as shown in Fig. P4–63 during the infinitesimal time period $dt = t_2 - t_1$. The velocity com-

ponents at point P at the initial time are u and v in the x- and y-directions, respectively. Show that the magnitude of the rate of rotation (angular velocity) about point P in the xy-plane is
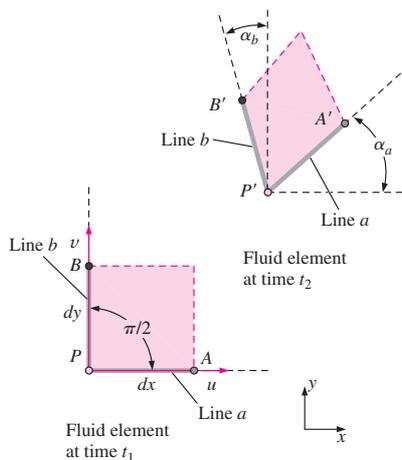
$$\omega_z = \frac{1}{2}\left(\frac{\partial v}{\partial x} - \frac{\partial u}{\partial y}\right)$$

4–64 A two-dimensional fluid element of dimensions dx and dy translates and distorts as shown in Fig. P4–63 during the infinitesimal time period $dt = t_2 - t_1$. The velocity components at point P at the initial time are u and v in the x- and y-directions, respectively. Consider the line segment PA in Fig. P4–63, and show that the magnitude of the linear strain rate in the x-direction is

$$\varepsilon_{xx} = \frac{\partial u}{\partial x}$$

4–65 A two-dimensional fluid element of dimensions dx and dy translates and distorts as shown in Fig. P4–63 during the infinitesimal time period $dt = t_2 - t_1$. The velocity components at point P at the initial time are u and v in the x- and y-directions, respectively. Show that the magnitude of the shear strain rate about point P in the xy-plane is

$$\varepsilon_{xy} = \frac{1}{2}\left(\frac{\partial u}{\partial y} + \frac{\partial v}{\partial x}\right)$$

4–66 Consider a steady, two-dimensional, incompressible flow field in the xy-plane. The linear strain rate in the x-direction is 2.5 s^{-1}. Calculate the linear strain rate in the y-direction.

4–67 A cylindrical tank of water rotates in solid-body rotation, counterclockwise about its vertical axis (Fig. P4–67) at angular speed $\dot{n} = 360$ rpm. Calculate the vorticity of fluid particles in the tank. *Answer: 75.4 $\vec{k}$ rad/s*
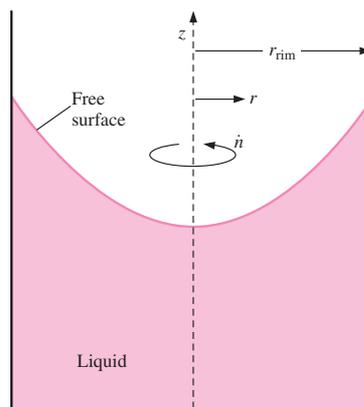
FIGURE P4–63

FIGURE P4–67

4–68 A cylindrical tank of water rotates about its vertical axis (Fig. P4–67). A PIV system is used to measure the vorticity field of the flow. The measured value of vorticity in the z-direction is -55.4 rad/s and is constant to within ± 0.5 percent everywhere that it is measured. Calculate the angular speed of rotation of the tank in rpm. Is the tank rotating clockwise or counterclockwise about the vertical axis?

4–69 A cylindrical tank of radius $r_{rim} = 0.35$ m rotates about its vertical axis (Fig. P4–67). The tank is partially filled with oil. The speed of the rim is 2.6 m/s in the counterclockwise direction (looking from the top), and the tank has been spinning long enough to be in solid-body rotation. For any fluid particle in the tank, calculate the magnitude of the component of vorticity in the vertical z-direction. *Answer:* 15.0 rad/s

4–70C Explain the relationship between vorticity and rotationality.

4–71 Consider a two-dimensional, incompressible flow field in which an initially square fluid particle moves and deforms. The fluid particle dimension is a at time t and is aligned with the x- and y-axes as sketched in Fig. P4–71. At some later time, the particle is still aligned with the x- and y-axes, but has deformed into a rectangle of horizontal length $2a$. What is the vertical length of the rectangular fluid particle at this later time?
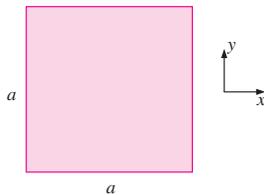
FIGURE P4–71

4–72 Consider a two-dimensional, *compressible* flow field in which an initially square fluid particle moves and deforms. The fluid particle dimension is a at time t and is aligned with the x- and y-axes as sketched in Fig. P4–71. At some later time, the particle is still aligned with the x- and y-axes but has deformed into a rectangle of horizontal length $1.06a$ and vertical length $0.931a$. (The particle's dimension in the z-direction does not change since the flow is two-dimensional.) By what percentage has the density of the fluid particle increased or decreased?

4–73 Consider the following steady, three-dimensional velocity field:

$$\vec{V} = (u, v, w)$$
$$= (3.0 + 2.0x - y)\vec{i} + (2.0x - 2.0y)\vec{j} + (0.5xy)\vec{k}$$

Calculate the vorticity vector as a function of space (x, y, z).

4–74 Consider fully developed **Couette flow**—flow between two infinite parallel plates separated by distance h, with the top plate moving and the bottom plate stationary as illustrated in Fig. P4–74. The flow is steady, incompressible, and two-dimensional in the xy-plane. The velocity field is given by

$$\vec{V} = (u, v) = V\frac{y}{h}\vec{i} + 0\vec{j}$$

Is this flow rotational or irrotational? If it is rotational, calculate the vorticity component in the z-direction. Do fluid particles in this flow rotate clockwise or counterclockwise? *Answers:* yes, $-V/h$, clockwise
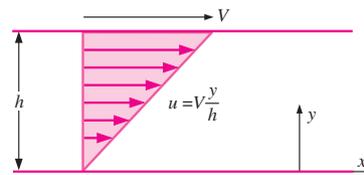
FIGURE P4–74

4–75 For the Couette flow of Fig. P4–74, calculate the linear strain rates in the x- and y-directions, and calculate the shear strain rate ε_{xy}.

4–76 Combine your results from Prob. 4–75 to form the two-dimensional strain rate tensor ε_{ij},

$$\varepsilon_{ij} = \begin{pmatrix} \varepsilon_{xx} & \varepsilon_{xy} \\ \varepsilon_{yx} & \varepsilon_{yy} \end{pmatrix}$$

Are the x- and y-axes principal axes?

Reynolds Transport Theorem

4–77C True or false: For each statement, choose whether the statement is true or false and discuss your answer briefly.

(*a*) The Reynolds transport theorem is useful for transforming conservation equations from their naturally occurring control volume forms to their system forms.

(*b*) The Reynolds transport theorem is applicable only to nondeforming control volumes.

(*c*) The Reynolds transport theorem can be applied to both steady and unsteady flow fields.

(*d*) The Reynolds transport theorem can be applied to both scalar and vector quantities.

4–78 Consider the general form of the Reynolds transport theorem (RTT) given by

$$\frac{dB_{sys}}{dt} = \frac{d}{dt}\int_{CV} \rho b\, dV + \int_{CS} \rho b\vec{V}_r \cdot \vec{n}\, dA$$

where $\vec{V}_r$ is the velocity of the fluid relative to the control surface. Let B_{sys} be the mass m of a system of fluid particles. We know that for a system, $dm/dt = 0$ since no mass can enter or leave the system by definition. Use the given equation to derive the equation of conservation of mass for a control volume.

4–79 Consider the general form of the Reynolds transport theorem (RTT) given by Prob. 4–78. Let B_{sys} be the linear momentum $m\vec{V}$ of a system of fluid particles. We know that for a system, Newton's second law is

$$\sum \vec{F} = m\vec{a} = m\frac{d\vec{V}}{dt} = \frac{d}{dt}(m\vec{V})_{sys}$$

Use the equation of Prob. 4–78 and this equation to derive the equation of conservation of linear momentum for a control volume.

4–80 Consider the general form of the Reynolds transport theorem (RTT) given in Prob. 4–78. Let B_{sys} be the angular momentum $\vec{H} = \vec{r} \times m\vec{V}$ of a system of fluid particles, where $\vec{r}$ is the moment arm. We know that for a system, conservation of angular momentum can be expressed as

$$\sum \vec{M} = \frac{d}{dt}\vec{H}_{sys}$$

where $\Sigma \vec{M}$ is the net moment applied to the system. Use the equation given in Prob. 4–78 and this equation to derive the equation of conservation of angular momentum for a control volume.

4–81 Reduce the following expression as far as possible:

$$F(t) = \frac{d}{dt}\int_{x=At}^{x=Bt} e^{-2x^2}\,dx$$

(Hint: Use the one-dimensional Leibnitz theorem.) *Answer: $Be^{-B^2t^2} - Ae^{-A^2t^2}$*

Review Problems

4–82 Consider fully developed two-dimensional **Poiseuille flow**—flow between two infinite parallel plates separated by distance h, with both the top plate and bottom plate stationary, and a forced pressure gradient dP/dx driving the flow as illustrated in Fig. P4–82. (dP/dx is constant and negative.)
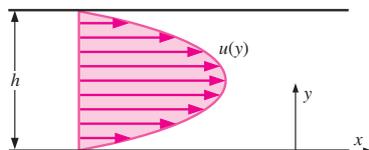
FIGURE P4–82

The flow is steady, incompressible, and two-dimensional in the xy-plane. The velocity components are given by

$$u = \frac{1}{2\mu}\frac{dP}{dx}(y^2 - hy) \qquad v = 0$$

where μ is the fluid's viscosity. Is this flow rotational or irrotational? If it is rotational, calculate the vorticity component in the z-direction. Do fluid particles in this flow rotate clockwise or counterclockwise?

4–83 For the two-dimensional Poiseuille flow of Prob. 4–82, calculate the linear strain rates in the x- and y-directions, and calculate the shear strain rate ε_{xy}.

4–84 Combine your results from Prob. 4–83 to form the two-dimensional strain rate tensor ε_{ij} in the xy-plane,

$$\varepsilon_{ij} = \begin{pmatrix} \varepsilon_{xx} & \varepsilon_{xy} \\ \varepsilon_{yx} & \varepsilon_{yy} \end{pmatrix}$$

Are the x- and y-axes principal axes?

4–85 Consider the two-dimensional Poiseuille flow of Prob. 4–82. The fluid between the plates is water at 40°C. Let the gap height $h = 1.6$ mm and the pressure gradient $dP/dx = -230$ N/m³. Calculate and plot seven *pathlines* from $t = 0$ to $t = 10$ s. The fluid particles are released at $x = 0$ and at $y = 0.2, 0.4, 0.6, 0.8, 1.0, 1.2,$ and 1.4 mm.

4–86 Consider the two-dimensional Poiseuille flow of Prob. 4–82. The fluid between the plates is water at 40°C. Let the gap height $h = 1.6$ mm and the pressure gradient $dP/dx = -230$ N/m³. Calculate and plot seven *streaklines* generated from a dye rake that introduces dye streaks at $x = 0$ and at $y = 0.2, 0.4, 0.6, 0.8, 1.0, 1.2,$ and 1.4 mm (Fig. P4–86). The dye is introduced from $t = 0$ to $t = 10$ s, and the streaklines are to be plotted at $t = 10$ s.
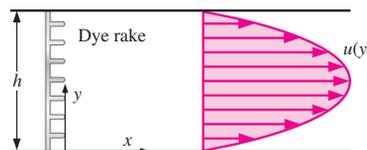
FIGURE P4–86

4–87 Repeat Prob. 4–86 except that the dye is introduced from $t = 0$ to $t = 10$ s, and the streaklines are to be plotted at $t = 12$ s instead of 10 s.

4–88 Compare the results of Probs. 4–86 and 4–87 and comment about the linear strain rate in the x-direction.

4–89 Consider the two-dimensional Poiseuille flow of Prob. 4–82. The fluid between the plates is water

at 40°C. Let the gap height $h = 1.6$ mm and the pressure gradient $dP/dx = -230$ N/m³. Imagine a hydrogen bubble wire stretched vertically through the channel at $x = 0$ (Fig. P4–89). The wire is pulsed on and off such that bubbles are produced periodically to create *timelines*. Five distinct timelines are generated at $t = 0, 2.5, 5.0, 7.5,$ and 10.0 s. Calculate and plot what these five timelines look like at time $t = 12.5$ s.
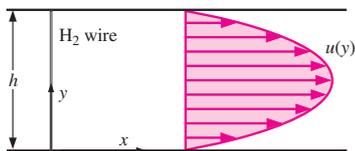
FIGURE P4–89

4–90 Consider fully developed axisymmetric Poiseuille flow—flow in a round pipe of radius R (diameter $D = 2R$), with a forced pressure gradient dP/dx driving the flow as illustrated in Fig. P4–90. (dP/dx is constant and negative.) The flow is steady, incompressible, and axisymmetric about the x-axis. The velocity components are given by

$$u = \frac{1}{4\mu}\frac{dP}{dx}(r^2 - R^2) \qquad u_r = 0 \qquad u_\theta = 0$$

where μ is the fluid's viscosity. Is this flow rotational or irrotational? If it is rotational, calculate the vorticity component in the circumferential (θ) direction and discuss the sign of the rotation.
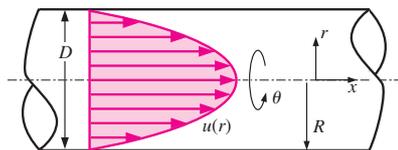
FIGURE P4–90

4–91 For the axisymmetric Poiseuille flow of Prob. 4–90, calculate the linear strain rates in the x- and r-directions, and calculate the shear strain rate ε_{xr}. The strain rate tensor in cylindrical coordinates (r, θ, x) and (u_r, u_θ, u_x), is

$$\varepsilon_{ij} = \begin{pmatrix} \varepsilon_{rr} & \varepsilon_{r\theta} & \varepsilon_{rx} \\ \varepsilon_{\theta r} & \varepsilon_{\theta\theta} & \varepsilon_{\theta x} \\ \varepsilon_{xr} & \varepsilon_{x\theta} & \varepsilon_{xx} \end{pmatrix}$$

$$= \begin{pmatrix} \dfrac{\partial u_r}{\partial r} & \dfrac{1}{2}\left(r\dfrac{\partial}{\partial r}\left(\dfrac{u_\theta}{r}\right) + \dfrac{1}{r}\dfrac{\partial u_r}{\partial \theta}\right) & \dfrac{1}{2}\left(\dfrac{\partial u_r}{\partial x} + \dfrac{\partial u_x}{\partial r}\right) \\ \dfrac{1}{2}\left(r\dfrac{\partial}{\partial r}\left(\dfrac{u_\theta}{r}\right) + \dfrac{1}{r}\dfrac{\partial u_r}{\partial \theta}\right) & \dfrac{1}{r}\dfrac{\partial u_\theta}{\partial \theta} + \dfrac{u_r}{r} & \dfrac{1}{2}\left(\dfrac{1}{r}\dfrac{\partial u_x}{\partial \theta} + \dfrac{\partial u_\theta}{\partial x}\right) \\ \dfrac{1}{2}\left(\dfrac{\partial u_r}{\partial x} + \dfrac{\partial u_x}{\partial r}\right) & \dfrac{1}{2}\left(\dfrac{1}{r}\dfrac{\partial u_x}{\partial \theta} + \dfrac{\partial u_\theta}{\partial x}\right) & \dfrac{\partial u_x}{\partial x} \end{pmatrix}$$

4–92 Combine your results from Prob. 4–91 to form the axisymmetric strain rate tensor ε_{ij},

$$\varepsilon_{ij} = \begin{pmatrix} \varepsilon_{rr} & \varepsilon_{rx} \\ \varepsilon_{xr} & \varepsilon_{xx} \end{pmatrix}$$

Are the x- and r-axes principal axes?

4–93 We approximate the flow of air into a vacuum cleaner attachment by the following velocity components in the centerplane (the xy-plane):

$$u = \frac{-\dot{V}x}{\pi L}\frac{x^2 + y^2 + b^2}{x^4 + 2x^2y^2 + 2x^2b^2 + y^4 - 2y^2b^2 + b^4}$$

and

$$v = \frac{-\dot{V}y}{\pi L}\frac{x^2 + y^2 - b^2}{x^4 + 2x^2y^2 + 2x^2b^2 + y^4 - 2y^2b^2 + b^4}$$

where b is the distance of the attachment above the floor, L is the length of the attachment, and $\dot{V}$ is the volume flow rate of air being sucked up into the hose (Fig. P4–93). Determine the location of any stagnation point(s) in this flow field.   *Answer: at the origin*
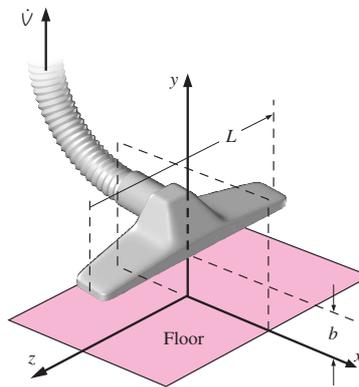
FIGURE P4–93

4–94 Consider the vacuum cleaner of Prob. 4–93. For the case where $b = 2.0$ cm, $L = 35$ cm, and $\dot{V} = 0.1098$ m³/s, create a velocity vector plot in the upper half of the xy-plane from $x = -3$ cm to 3 cm and from $y = 0$ cm to 2.5 cm. Draw as many vectors as you need to get a good feel of the flow field. *Note*: The velocity is infinite at the point $(x, y) = (0, 2.0$ cm), so do not attempt to draw a velocity vector at that point.

4–95 Consider the approximate velocity field given for the vacuum cleaner of Prob. 4–93. Calculate the flow speed along the floor. Dust particles on the floor are most likely to be sucked up by the vacuum cleaner at the location of maxi-

mum speed. Where is that location? Do you think the vacuum cleaner will do a good job at sucking up dust directly below the inlet (at the origin)? Why or why not?

4–96 Consider a steady, two-dimensional flow field in the xy-plane whose x-component of velocity is given by

$$u = a + b(x - c)^2$$

where a, b, and c are constants with appropriate dimensions. Of what form does the y-component of velocity need to be in order for the flow field to be incompressible? In other words, generate an expression for v as a function of x, y, and the constants of the given equation such that the flow is incompressible. *Answer: $-2b(x - c)y + f(x)$*

4–97 There are numerous occasions in which a fairly uniform free-stream flow encounters a long circular cylinder aligned normal to the flow (Fig. P4–97). Examples include air flowing around a car antenna, wind blowing against a flag pole or telephone pole, wind hitting electrical wires, and ocean currents impinging on the submerged round beams that support oil platforms. In all these cases, the flow at the rear of the cylinder is separated and unsteady, and usually turbulent. However, the flow in the front half of the cylinder is much more steady and predictable. In fact, except for a very thin boundary layer near the cylinder surface, the flow field may be approximated by the following steady, two-dimensional velocity components in the xy- or $r\theta$-plane:

$$u_r = V \cos \theta \left(1 - \frac{a^2}{r^2} \right) \qquad u_\theta = -V \sin \theta \left(1 + \frac{a^2}{r^2} \right)$$
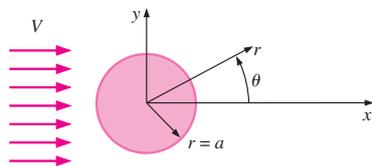
FIGURE P4–97

Is this flow field rotational or irrotational? Explain.

4–98 Consider the flow field of Prob. 4–97 (flow over a circular cylinder). Consider only the front half of the flow ($x < 0$). There is one stagnation point in the front half of the flow field. Where is it? Give your answer in both cylindrical (r, θ) coordinates and Cartesian (x, y) coordinates.

4–99 Consider the upstream half ($x < 0$) of the flow field of Prob. 4–97 (flow over a circular cylinder). We introduce a parameter called the **stream function** ψ, which is *constant along streamlines* in two-dimensional flows such as the one being considered here (Fig. P4–99). The velocity field of Prob. 4–97 corresponds to a stream function given by

$$\psi = V \sin \theta \left(r - \frac{a^2}{r} \right)$$

(*a*) Setting ψ to a constant, generate an equation for a streamline. (Hint: Use the quadratic rule to solve for r as a function of θ.)

(*b*) For the particular case in which $V = 1.00$ m/s and cylinder radius $a = 10.0$ cm, plot several streamlines in the upstream half of the flow ($90° < \theta < 270°$). For consistency, plot in the range -0.4 m $< x < 0$ m, -0.2 m $< y < 0.2$ m, with stream function values evenly spaced between -0.16 m²/s and 0.16 m²/s.
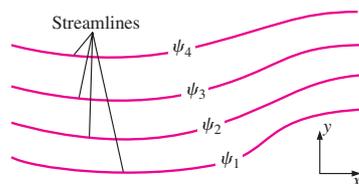
FIGURE P4–99

4–100 Consider the flow field of Prob. 4–97 (flow over a circular cylinder). Calculate the two linear strain rates in the $r\theta$-plane; i.e., calculate ε_{rr} and $\varepsilon_{\theta\theta}$. Discuss whether fluid line segments stretch (or shrink) in this flow field. (Hint: The strain rate tensor in cylindrical coordinates is given in Prob. 4–91.)

4–101 Based on your results of Prob. 4–100, discuss the compressibility (or incompressibility) of this flow. *Answer: flow is incompressible*

4–102 Consider the flow field of Prob. 4–97 (flow over a circular cylinder). Calculate $\varepsilon_{r\theta}$, the shear strain rate in the $r\theta$-plane. Discuss whether fluid particles in this flow deform with shear or not. (Hint: The strain rate tensor in cylindrical coordinates is given in Prob. 4–91.)